Engineering Reports

WILEY

Engineering Reports Open Access

RESEARCH ARTICLE OPEN ACCESS

Novel Unit Distribution for Enhanced Modeling Capabilities: Healthcare and Geological Applications

Amal S. Hassan[1] | Gaber Sallam Salem Abdalla[2] | Abdoulie Faal[3] | Omar A. Saudi[4]

[1]Faculty of Graduate Studies for Statistical Research, Cairo University, Giza, Egypt | [2]Department of Insurance and Risk Management, Faculty of Business, Imam Mohammad Ibn Saud Islamic University (IMSIU), Riyadh, Saudi Arabia | [3]Mathematics Unit, Department Physical and Natural Sciences, School of Arts and Sciences, University of The Gambia, The Gambia | [4]Department of Basic Sciences, Higher Institute of Management Sciences (HIMS), Cairo, Egypt

Correspondence: Abdoulie Faal (faala2520@gmail.com)

Received: 25 April 2025 | **Revised:** 8 June 2025 | **Accepted:** 25 June 2025

Funding: This work was supported and funded by the Deanship of Scientific Research at Imam Mohammad Ibn Saud Islamic University (IMSIU) (grant number IMSIU-DDRSP2501).

Keywords: inverse exponentiated Pareto distribution | Kolmogorov method | Rényi entropy | stochastic ordering

ABSTRACT

In statistical modeling, unit distributions are essential for evaluating proportional or rate-based data in domains including public health, environmental science, and finance. While there are many different unit distributions, a scalable model is required to capture unique features in various data environments. This article introduces the unit inverse exponentiated Pareto (UIEP) distribution, a novel two-parameter model. Unimodal, inverted J-shaped, left-skewed, and right-skewed probability density functions, as well as rising, J-shaped, or U-shaped hazard rate functions, are some of the different shapes of the UIEP. Because of these adaptable features, it is more suited for unit data modeling. Stochastic ordering, quantiles, moments, probability-weighted moments, significant uncertainty measures, Lorenz and Bonferroni curves, and stress-strength reliability are among the key statistical features that are analytically generated. Statistical inference employed a number of methods, such as maximum likelihood, weighted least squares, Anderson-Darling, least squares, and Kolmogorov, to estimate distribution parameters and assess different entropy measures. These statistical techniques make up an effective tool for academics and data analysts. Among these, simulation results indicated that the Kolmogorov method was the most effective for parameter estimation, particularly when combined with Arimoto, Rényi, Havrda-Charvát, and Tsallis entropy measures. Furthermore, for low and high entropy orders, respectively, Arimoto and Rényi entropies performed better when maximum likelihood estimation was used. This result demonstrates a strong correlation between the most efficient estimator and the entropy order. Our results show that both the absolute bias and the mean squared error consistently decrease as the sample size increases. This pattern confirms that the provided estimation methods are reliable and consistent. To validate the proposed distribution, we applied it to two real-world datasets: health data related to COVID-19 and geological data from petroleum rock samples. These applications demonstrated improved model fit compared to alternative distributions.

1 | Introduction

The literature has lately suggested a wide range of statistical distributions as alternatives for the current models. Creating new distributions is primarily done to provide more flexibility in modeling and capturing the statistical features of real-world data. In order to enhance the field, a lot of academics work to introduce novel distributions. One efficient method for generating new distributions is the inverse transformation method applied to a baseline variable. Distributions using this method frequently have a parsimonious parameter structure. Inverse distributions are essential for statistical modeling and analysis, especially when working with skew or heavy-tailed data. An inverse transformation is used to generate these distributions. Specifically, if X represents the baseline distribution and Y is defined as the reciprocal of X (i.e., $Y = 1/X$), then the resulting new distribution of the random variable Y exhibits distinct characteristics. Often, this transformation is required in order to precisely model the special characteristics of particular datasets, including those found in industries like reliability engineering, insurance, and finance. Some of the suggested inverted distributions are the inverse Lindley distribution [1], the inverse power Lindley distribution ([2], the inverse exponentiated Weibull distribution [3], the inverse Nakagami-m distribution [4], the inverse Kumaraswamy (KW) distribution [5], the inverse power Lomax distribution [6], the inverse Nadarajah–Haghighi distribution [7], the inverse exponentiated Lomax distribution [8], the inverse xgamma distribution [9], the inverse Weibull generator [10, 11], the inverse Maxwell distribution [12], the inverse Topp-Leone distribution [13], the inverse Pareto distribution [14], the inverse Ishita distribution [15], the inverse-power logistic-exponential distribution [16], the inverse power Cauchy distribution [17], the inverse power Ramos-Louzada distribution [18], the inverse Shanker distribution [19], the sine inverse exponentiated Weibull distribution [20], the inverse power Zeghdoudi distribution [21], and the arcsine inverse Weibull generator [22], among others.

This study focuses on the inverse exponentiated Pareto (IEP) distribution introduced by Ghitany et al. [23]. The IEP distribution is the inverse form of the exponentiated Pareto distribution (Gupta et al. [24]). The probability density function (PDF) of the IEP distribution is given by:

$$f(x) = \delta_1 \delta_2 x^{\delta_2 - 1} \ (1+x)^{-(\delta_2+1)} \left[1 - \left(1 + \frac{1}{x}\right)^{-\delta_2}\right]^{\delta_1 - 1}; \ x > 0, \quad (1)$$

where $\delta_1 > 0$ and $\delta_2 > 0$ are the shape parameters. The cumulative distribution function (CDF) is

$$F(x) = 1 - \left[1 - \left(1 + \frac{1}{x}\right)^{-\delta_2}\right]^{\delta_1}; \ x > 0. \quad (2)$$

The IEP distribution's hazard rate function (HRF) is notably flexible, capable of displaying increasing, decreasing, reversed J-shaped, upside-down, or non-monotonic characteristics. The IEP distribution is a good paradigm for lifetime and reliability modeling with a broad variety of potential applications ranging from analysis of fatigue failure and degradation tests to mechanical, electrical, and even mortality data estimation. Its properties align with other popular distributions like the generalized exponential, exponentiated moment exponential, and inverse exponential Rayleigh distributions, as mentioned by Pradhan and Kundu [25]. Recent work keeps on enhancing its application; for example, Maurya et al. [26] discussed the estimation of parameters under Type-II progressive censoring. Shaikh and Patel [27] focused on estimation via record values. The multicomponent stress-strength reliability (S-SR) estimation under censored samples was examined by [28, 29].

Distributions with support limited to the interval [0, 1] have grown significantly in the last few years. As fractions, rates, or percentages, these distributions are essential for modeling data in this range. This type of data is commonly encountered in many disciplines, such as risk analysis, psychology, economics, medicine, and engineering. Regression, semiparametric, and parametric model building are highly desired in order to examine this data efficiently across a variety of application fields. Notably, a significant portion of today's unit distributions are derived by appropriately transforming existing distributions with support $(0,\infty)$. As a result, several different unit distributions have been created. The unit Lindley distribution [30], the unit-Gompertz distribution [31, 32], the unit-Weibull distribution [33], the unit exponentiated half logistic (UEHL) distribution [34], the unit modified Burr-III distribution [35], the unit exponentiated Lomax (UEL) distribution [36], the unit generalized half normal distribution [37], the unit log logistic (ULL) distribution [38], the unit power-skew-normal distribution [39], the unit inverse exponentiated Weibull distribution [40], the unit Burr-XII distribution [41], the unit-power Burr X unit distribution [42], the unit half-logistic geometric distribution [43], the unit xgamma distribution [44], the unit power Lomax (UPL) distribution [45], the unit Teissier distribution [46], the mixture of log-Bilal distributions [47], the generalized exponentiated unit Gompertz [48], the unit Gumbel Type-II distribution [49], the half-logistic unit-Gompertz Type-I distribution [50], the unit Bilal distribution [51], and the unit inverse power Lomax distribution [52] are noteworthy examples.

This work introduces a UIEP distribution, a newly developed unit probability distribution from the IEP. The proposed two-parameter UIEP distribution is derived by using the transformation $Y = \frac{1}{1+X}$ where X is an IEP distribution with PDF (1) and CDF(2). The following are the reasons that inspired us to introduce the UIEP distribution:

- The UIEP distribution shows high flexibility and can model different datasets with values ranging between zero and one. Its density function takes on diverse shapes, including unimodal, reversed J-shaped, left-skewed, and right-skewed. The UIEP hazard function may have increasing, J-shaped, or bathtub hazard rate patterns.
- Explore a number of statistical structure, including moments, quantile function (QF), incomplete moments (IMs), stochastic ordering (SO), probability- weighted moments (PWM), some measures of uncertainty, and S-SR.
- To discuss the challenges of estimating the model parameters with certain uncertainty measures, i.e., Rényi (Ré), Havrda and Charvát (H–C), Tsallis (TS), and Arimoto (AR).
- The UIEP distribution estimators are discussed utilizing some estimation techniques like the maximum likelihood

(ML), least squares (LS), Kolmogorov (KO), weighted LS (WLS), and Anderson–Darling (AD).

- To assess the performance and accuracy of the suggested parameter and entropies estimation techniques, a comprehensive simulation study is carried out.
- Statistically, compared with other rival models, the UIEP model has been compared with some well-known distributions, including unit exponential Pareto (UEP) distribution, UEL distribution, UEHL distribution, KW distribution, and exponentiated Topp-Leone (ETL) distribution.

The remaining parts of this paper's sections are structured as follows: Section 2 gives the description of the UIEP distribution. Section 3 presents the statistical properties of the UIEP distribution, i.e., QF, PWM, moments, IMs, Lorenz and Bonferroni curves, SO, and S-SR. Section 4 gives expressions for the proposed entropy measures. Section 5 discusses the estimation of UIEP distribution parameters and gives estimators of the proposed entropy measures. Section 6 gives an overview of the simulation study, and Monte Carlo simulation was utilized to compare different results of entropy estimates. Two real datasets in Section 7 demonstrate the UIEP distribution's flexibility and usefulness. The paper finally concludes with an overview of the main conclusions and findings in Section 8.

2 | The Unit Inverse Exponentiated Pareto Distribution

This section's goal is to determine the UIEP's PDF and CDF. It explores the survival function, HRF, and reversed HRF. Also, it includes a graphical representation of both the PDF and HRF of the UIEP distribution.

The UIEP distribution is derived by applying the transformation to a random variable X following the IEP distribution. Specifically, $Y = \frac{1}{1+X}$, where X has the CDF of the IEP distribution given in Equation (2). The resulting CDF of the UIEP distribution is derived as follows:

$$H(y) = P(Y \le y) = P(1 \le y + yX) = P\left(\frac{1-y}{y} \le X\right)$$
$$= 1 - P\left(X \le \frac{1-y}{y}\right) = 1 - H_X\left(\frac{1-y}{y}\right), \tag{3}$$

then,

$$H_X\left(\frac{1-y}{y}\right) = 1 - \left[1 - \left(1 + \frac{y}{1-y}\right)^{-\delta_2}\right]^{\delta_1}$$
$$= 1 - \left[1 - \left(\frac{1}{1-y}\right)^{-\delta_2}\right]^{\delta_1} = 1 - \left[1 - (1-y)^{\delta_2}\right]^{\delta_1}. \tag{4}$$

Then, from Equations (3 and 4), the CDF of the UIEP distribution, with shape parameters $\delta_1 > 0$ and $\delta_2 > 0$, is given by:

$$H(y) = \left[1 - (1-y)^{\delta_2}\right]^{\delta_1}; \quad \delta_1, \delta_2 > 0, y \in (0,1), \tag{5}$$

where $H(y) = 0$, for $y \le 0$, and $H(y) = 1$, for $y \le 1$. The PDF of the UIEP distribution is as below:

$$h(y) = \delta_1\delta_2(1-y)^{\delta_2-1}\left[1-(1-y)^{\delta_2}\right]^{\delta_1-1}; \delta_1, \delta_2 > 0, y \in (0,1), \tag{6}$$

and $h(y) = 0$ for $y \notin [0,1]$. A random variable with PDF (6) is represented by UIEP (δ_1, δ_2). For $\delta_1 = 1$, the PDF (6) provides the unit inverse Pareto distribution as a new sub-model.

The survival function, HRF, and cumulative HRF (for $y \in (0,1)$) are, respectively, given by:

$$\overline{H}(y) = 1 - \left[1-(1-y)^{\delta_2}\right]^{\delta_1},$$
$$z(y) = \frac{\delta_1\delta_2(1-y)^{\delta_2-1}\left[1-(1-y)^{\delta_2}\right]^{\delta_1-1}}{1-\left[1-(1-y)^{\delta_2}\right]^{\delta_1}}, \tag{7}$$

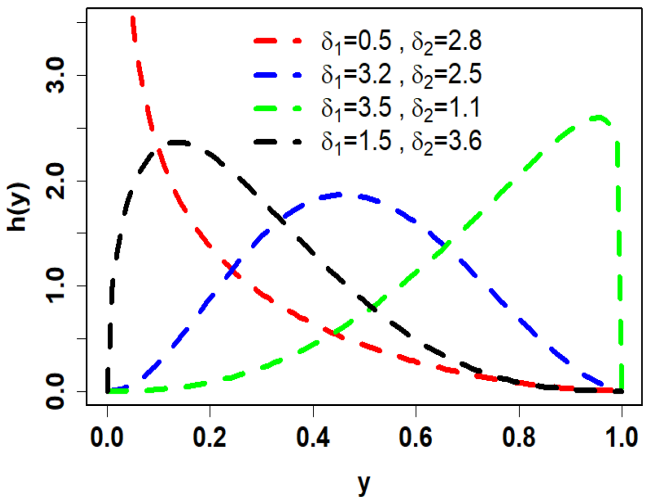

FIGURE 1 | Shapes of the PDF of the UIEP distribution for varying parameter values.

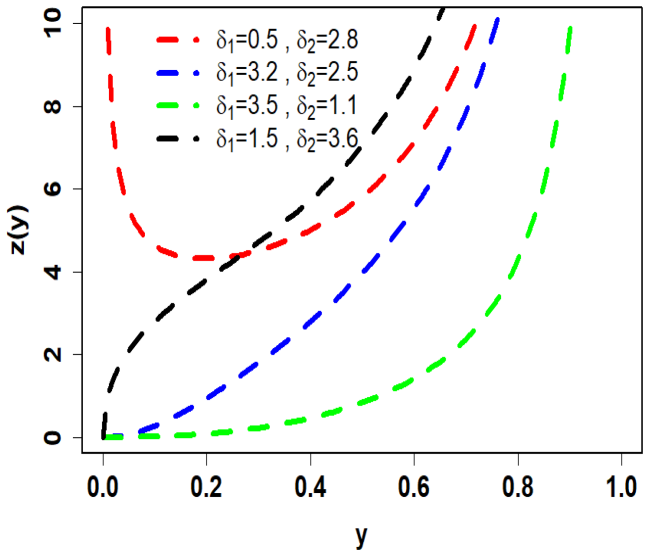

FIGURE 2 | Shapes of the HRF of the UIEP distribution for varying parameter values.

and,

$$\kappa(y) = -\log\left[1-\left[1-(1-y)^{\delta_2}\right]^{\delta_1}\right].$$

To visualize the shapes of the PDF (6) and HRF (7), Figures 1 and 2 depict their plots for varying values of the parameters δ_1 and δ_2. The PDF graphs, in Figure 1, for different combinations of parameters show a range of shapes, including reversed J-shaped, left-skewed, right-skewed, and unimodal. Significantly, depending on the parameter values, the HRF exhibits remarkable flexibility, showing growing, decreasing, bathtub, and j-shaped patterns (see Figure 2). This illustrates the great level of flexibility needed for various unit data analysis.

3 | Characteristics of UIEP Distribution

Several important statistical properties of the UIEP distribution are examined in this section. Moments, IMs, QF, SO, PWM, and S-SR are some of these properties.

3.1 | Probability Weighted Moments

Greenwood et al. [53] first proposed the idea of the PWM, which has since led to a major advance in parameter estimation for a variety of probability distributions. The PWM is typically favored over ordinary moments when dealing with distributions that exhibit heavy tails or extreme values. The PWM is less sensitive to extreme values. According to Ref. [53], the class of PWM, for a random variable Y with a real number l and h, is defined as follows:

$$\eta_{l,h} = E\left[Y^l H(y)^h\right] = \int_{-\infty}^{\infty} y^l (H(y))^h h(y) dy. \tag{8}$$

The PWM of the UIEPL distribution is given by inserting CDF (5) and the PDF (6) in Equation (8).

$$\eta_{l,h} = \int_0^1 y^l \delta_1 \delta_2 (1-y)^{\delta_2-1}\left[1-(1-y)^{\delta_2}\right]^{h\delta_1+\delta_1-1} dy. \tag{9}$$

Using the binomial expansion

$$(1-u)^v = \sum_{j=0}^{\infty}\binom{v}{j}(-1)^j u^j, \qquad |u|<1, \tag{10}$$

in Equation (9), then we have

$$\eta_{l,h} = \sum_{j=0}^{\infty}(-1)^j \delta_1\delta_2\binom{\delta_1(h+1)-1}{j} B\big(l+1, \delta_2(j+1)\big),$$

where B (.,.) is the beta function.

3.2 | Moments Measures

To comprehend the essential characteristics of a distribution, it is essential to look at moments and related measures. They offer important insights into shape, dispersion, and central tendency, all of which are essential for efficient statistical analysis and hypothesis testing. The m^{th} moment of the UIEP distribution is derived as

$$\mu'_m = \delta_1\delta_2\int_0^1 y^m (1-y)^{\delta_2-1}\left[1-(1-y)^{\delta_2}\right]^{\delta_1-1} dy. \tag{11}$$

Using the binomial expansion (10) in Equation (11) gives

$$\mu'_m = \delta_1\delta_2\sum_{j=0}^{m}(-1)^j\binom{\delta_1-1}{j} B\big(m+1, \delta_2(j+1)\big),$$

where, B(.,.) is the beta function. Furthermore, the m^{th} central moment of a given random variable Y is defined by

$$\mu_m = E\big(Y-\mu'_1\big)^m = \sum_{h=0}^{m}(-1)^h\binom{m}{h}\big(\mu'_1\big)^h \mu'_{m-h}.$$

Numerical values for certain parameter values, (a) $\big(\delta_1=0.5, \delta_2=0.5\big)$, (b) $\big(\delta_1=0.5, \delta_2=1.5\big)$, (c) $\big(\delta_1=0.5, \delta_2=2\big)$, (d) $\big(\delta_1=0.5, \delta_2=3\big)$ of the first four moments $\big(\mu'_1, \mu'_2, \mu'_3, \mu'_4\big)$ variance (σ^2), coefficient of Skewness (CS) and coefficient of Kurtosis (CK) of the UIEL distribution are listed in Table 1.

Table 1 shows that the moment values increase, but the CS and σ^2 values decrease when δ_1 increases and δ_2 keeps constant. Both platykurtic and leptokurtic distributions, as well as left- and right-skewed distributions, are possible for the UIEP. Figure 3 displays these patterns for 3D plots of μ'_1, σ^2, CS, and CK.

TABLE 1 | Some moments of UIEP distribution.

Measures		Parameters						
δ_1	δ_2	μ'_1	μ'_2	μ'_3	μ'_4	σ^2	CS	CK
0.5	0.5	0.4667	0.3397	0.2781	0.2403	0.1219	0.1353	1.5386
	1.5	0.2608	0.1335	0.0847	0.0600	0.0655	0.9396	2.8384
	2	0.2146	0.0959	0.0548	0.0355	0.0498	1.1513	3.4939
	3	0.1587	0.0566	0.0269	0.0150	0.0314	1.4389	4.6253
3	0.5	0.9000	0.8286	0.7738	0.7299	0.0186	−2.1073	7.8661
	1.5	0.6318	0.4417	0.3295	0.2573	0.0425	−0.3642	2.3694
	2	0.5429	0.3357	0.2262	0.1619	0.0410	−0.0711	2.2658
	3	0.4214	0.2110	0.1188	0.0728	0.0334	0.2798	2.4776

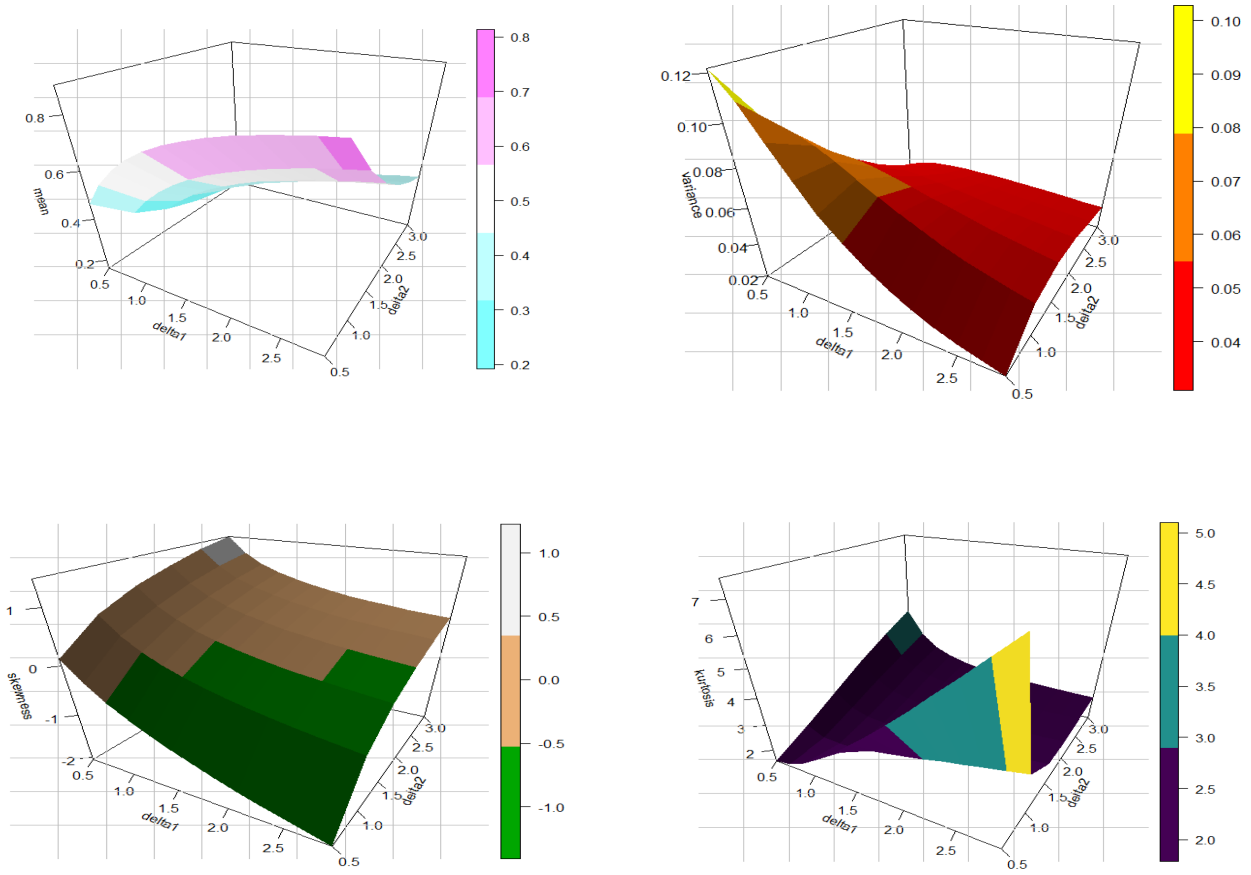

FIGURE 3 | The 3D plots for UIEP distribution of mean, variance, skewness, and kurtosis.

Figure 3 shows how the UIEP distribution is flexible in skewness and kurtosis. The skewness ranges from about −2 to 1, showing a wide variety of options. Furthermore, kurtosis can have both small and large values, allowing the distribution to display all three kurtosis types: leptokurtic, mesokurtic, and platykurtic. These results show how the PDF and HRF of the UIEP distribution may take on various forms.

3.3 | Incomplete Moments

A distribution's IM offers important information beyond just means and variances. They highlight extreme occurrences by capturing the dynamics of tails and asymmetries. For thorough risk assessment and decision-making, this knowledge is essential. We can improve the efficacy of our statistical analysis and obtain a deeper knowledge of the underlying data by accepting IMs.

The m^{th} IM of the UIEP distribution is derived as

$$\mu'_m(t) = \delta_1\delta_2\int_0^t y^m(1-y)^{\delta_2-1}\left[1-(1-y)^{\delta_2}\right]^{\delta_1-1}dy. \tag{12}$$

Using the binomial expansion (10) in Equation (12) gives

$$\mu'_m = \delta_1\delta_2\sum_{j=0}^{m}(-1)^j\binom{\delta_1-1}{j}B\big(m+1,\delta_2(j+1),t\big),$$

where $B(.,.,x)$ is the incomplete beta function. The Lorenz curve given by $L_F(t) = \mu'_1(t)/\mu'_1$ and the Bonferroni curve given by and $B_F(t) = L(t)/H(t)$, respectively, are notable applications of the first IM. These curves have significant utility in various fields, including economics, demographics, insurance, engineering, and medicine, for analyzing inequality, wealth distribution, and other crucial aspects.

Figure 4 shows inequality differences between the Lorenz and Bonferroni curves for five groups that have different δ_1 and δ_2 values. The green curve, which represents the greatest inequality, is the farthest off the equality line in the Lorenz plot and has the lowest Bonferroni curve, particularly in the lower tail, showing that the lowest 20% of the population receives the smallest amount of income. Conversely, the gold curve displays the lowest inequality, with both curves closer to the equality line, showing a more balanced income distribution. Cods of Lorenz and Bonferroni curves are given in Appendix B.

3.4 | Quantile Function

The QF of the UIEP distribution, for $p\in(0,1)$, is derived by inverting its CDF (5) as follows:

$$Q(p) = 1-\left(1-(p)^{1/\delta_1}\right)^{1/\delta_2}.$$

The QF yields a number of important statistical metrics. For instance, at $p=0.5$ gives the median (second quartile, denoted as

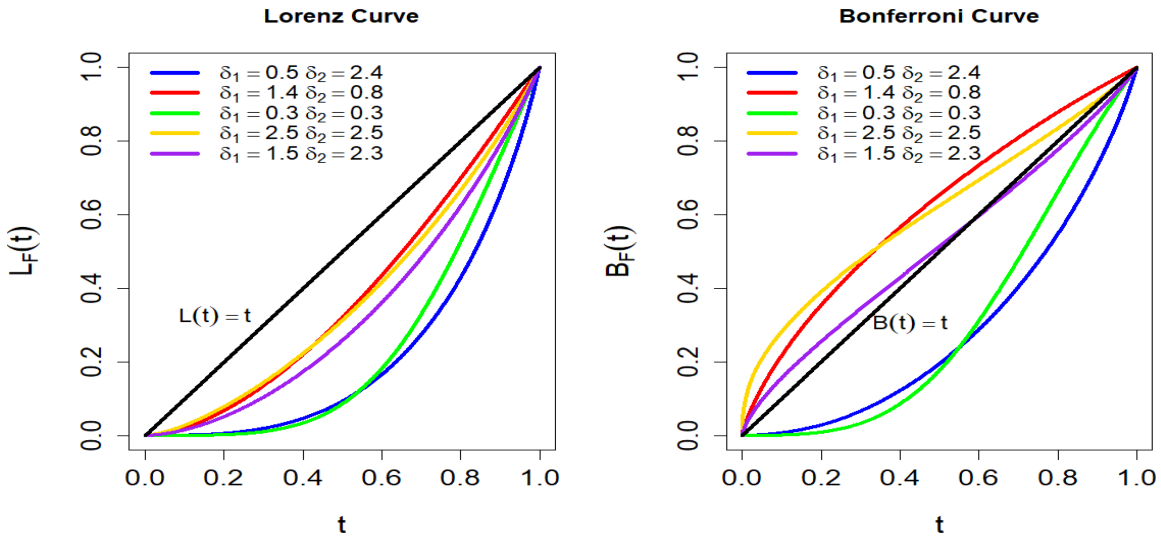

FIGURE 4 | Lorenz and Bonferroni curves of the UIEP distribution.

Q_2), while at $p = 0.75$ provides the third quartile (denoted by Q_3) and at $p = 0.25$ gives the first quartile (denoted by Q_1). We can use the following expression to create the random numbers for the UIEP distribution.

$$y_p = 1 - \left(1 - (p)^{1/\delta_1}\right)^{1/\delta_2}.$$

3.5 | Stochastic Ordering

A foundational idea in probability theory, SO has been studied and used extensively for more than 40 years. Numerous domains, such as biological sciences, economics, insurance, survival analysis, queueing theory, and reliability engineering, find use for it. A useful tool for evaluating the robustness and performance of system components, this framework allows the comparison of non-negative continuous random variables.

Let Y_1 has the UIEP (δ_1, δ_2) with PDF $h_1(y)$ and Y_2 has the UIEP (δ_3, δ_4) with PDF $h_2(y)$. In terms of likelihood ratio order; Y_1 is said to be stochastically less than Y_2 (written as $Y_1 \leq_{lr} Y_2$) if $h_1(y)/h_2(y)$ is a decreasing function $\forall y$. The following is likelihood ratio ordering:

$$\frac{h_1(y)}{h_2(y)} = \frac{\delta_1\delta_2(1-y)^{\delta_2-1}\left[1-(1-y)^{\delta_2}\right]^{\delta_1-1}}{\delta_3\delta_4(1-y)^{\delta_4-1}\left[1-(1-y)^{\delta_4}\right]^{\delta_3-1}}.$$

It is obtained $\frac{d}{dy}\left[\log\left(h_1(y)/h_2(y)\right)\right] < 0$, at $\delta_1 > \delta_3$ and $\delta_2 > \delta_4, \forall y \geq 0$, hence $\frac{d}{dy}\left[\log\left(h_1(y)/h_2(y)\right)\right] < 0$ is a decreasing function $\forall y$ and hence $Y_1 \leq_{Ir} Y_2$. Conclusions can also be made for various SO, like: hazard rate order $(Y_1 \leq_{hr} Y_2)$, mean residual life order $(Y_1 \leq_{mrl} Y_2)$, SO $(Y_1 \leq_{st} Y_2)$, and reversed hazard rate order $(Y_1 \leq_{rhr} Y_2)$.

3.6 | Stress-Strength Model

This subsection establishes the S-SR parameter for the UIEP model. The S-SR model is a popular method for estimating reliability that has important uses in many fields of physics and engineering. The mathematical expression for reliability (R) in this model is $R = P_r(Y_2 < Y_1)$, which is a probability that the system's strength (Y_1) will be greater than the enforced stress (Y_2). When the applied stress exceeds the system's strength $(Y_2 > Y_1)$, the system fails. On the other hand, when $Y_1 > Y_2$, the component performs adequately. In electrical and electronic systems, reliability (R) is especially significant as a metric for system performance. It can also be thought of as a probability that the system is strong enough to bear the stress that has been applied to it. Suppose that Y_1 is the strength random variable having UIEP (δ_1, δ_2) and Y_2 is the stress random variable having UIEP (δ_3, δ_2), where Y_1 and Y_2 are independent; the S-SR can be determined as follows:

$$R = \int_0^1 \delta_1\delta_2(1-y)^{\delta_2-1}\left[1-(1-y)^{\delta_2}\right]^{\delta_1+\delta_3-1}dy = \frac{\delta_1}{\delta_1+\delta_3}. \quad (13)$$

Note that the formula of S-SR of the UIEP given in Equation (13) is a function of the parameters (δ_1, δ_3).

4 | Information Measures

Entropy, an essential idea in information theory, quantifies the uncertainty associated with a random variable. It determines how much information should be present in that variable. In many disciplines, such as statistics, physics, chemistry, economics, insurance, finance, and biological sciences, entropy is essential. Entropy often increases with decreasing information content in a sample. This section gives, expressions of some entropy measures, including Ré, H–C, TS, and AR. The Ré entropy of order b, presented by Rényi [54], is defined by.

$$\chi_1 = \frac{1}{1-b}\log\left[\int_{-\infty}^{\infty} h(y)^b dy\right], b > 0, b \neq 1. \quad (14)$$

Inserting PDF (6) in Equation (14), then the Ré entropy of the UIEP distribution is obtained as follows:

$$\chi_1 = \frac{1}{1-b}\log\left[\int_0^1 \left(\delta_1\delta_2\right)^b (1-y)^{b(\delta_2-1)}\left[1-(1-y)^{\delta_2}\right]^{b(\delta_1-1)}dy\right]. \quad (15)$$

Using the transformation $z = (1-y)^{\delta_2} \Rightarrow dz = -\delta_2(1-y)^{\delta_2-1}dy$ in Equation (15) gives

$$\chi_1 = \frac{1}{1-b}\log\left[\delta_1^b\delta_2^{b-1}\mathrm{B}\left(\frac{b(\delta_2-1)}{\delta_2}+\frac{1}{\delta_2}, b(\delta_1-1)+1\right)\right], \tag{16}$$

where $B(.,.)$ is the beta function. The H–C entropy measure, presented by Ref. [55], is defined by:

$$\chi_2 = \frac{1}{2^{1-b}-1}\left[\int_{-\infty}^{\infty} h(y)^b dy - 1\right], b > 0, b \neq 1. \tag{17}$$

Inserting PDF(6) in Equation (17) and using the transformation $z = (1-y)^{\delta_2}$, then the H–C entropy of the UIEP distribution is obtained as follows:

$$\chi_2 = \frac{1}{2^{1-b}-1}\left[\delta_1^b\delta_2^{b-1}\mathrm{B}\left(\frac{b(\delta_2-1)}{\delta_2}+\frac{1}{\delta_2}, b(\delta_1-1)+1\right)-1\right], \tag{18}$$

where $B(.,.)$ is the beta function. The TS entropy measure, presented by Tsallis [56], is defined by:

$$\chi_3 = \frac{1}{b-1}\left[1-\int_{-\infty}^{\infty} h(y)^b dy\right]; b > 0, b \neq 1. \tag{19}$$

Inserting PDF(6) in Equation (19) and using the transformation $z = (1-y)^{\delta_2}$, then the TS entropy of the UIEP distribution is obtained as follows:

$$\chi_3 = \frac{1}{b-1}\left[1-\delta_1^b\delta_2^{b-1}\mathrm{B}\left(\frac{b(\delta_2-1)}{\delta_2}+\frac{1}{\delta_2}, b(\delta_1-1)+1\right)\right], \tag{20}$$

where $B(.,.)$ is the beta function. The AR entropy measure, presented by Arimoto [57], is defined by

$$\chi_4 = \frac{b}{b-1}\left[\left(\int_{-\infty}^{\infty} h(y)^b dy\right)^{1/b} - 1\right]; b > 0, b \neq 1. \tag{21}$$

Inserting PDF (4) of the UIEP distribution in Equation (21) and using the transformation $z = (1-y)^{\delta_2}$, then the AR entropy is obtained as follows

$$\chi_4 = \frac{b}{b-1}\left[\left(\delta_1^b\delta_2^{b-1}\mathrm{B}\left(\frac{b(\delta_2-1)}{\delta_2}+\frac{1}{\delta_2}, b(\delta_1-1)+1\right)\right)^{1/b} - 1\right], \tag{22}$$

where $B(.,.)$ is the beta function.

5 | Estimation Methods

In order to estimate parameters for the UIEP distribution, this section looks at five distinct approaches: ML, KO, AD, WLS, and LS. It also investigates the estimation of four entropy metrics for the UIEP distribution: AR, TS, Ré, and H–C. Each of these methods provides a unique method for estimating entropy measures and model parameters.

5.1 | Maximum Likelihood Method

To estimate the unknown parameters and entropy measures of the UIEP distribution, the ML technique is used. Consider an observed simple random sample of size n, denoted by $y_1, y_2, \ldots, y_n$ taken from the UIEP distribution. The log-likelihood function of the observed sample is given by

$$l^* = n\log(\delta_1\delta_2) + (\delta_2-1)\sum_{i=1}^{n}\log(1-y_i) + (\delta_1-1)\sum_{i=1}^{n}\log\left[1-(1-y_i)^{\delta_2}\right].$$

The ML estimators of δ_1 and δ_2 can be determined by solving the following two non-linear equations:

$$\frac{\partial l^*}{\partial \delta_1} = \frac{n}{\delta_1} + \sum_{i=1}^{n}\log\left[1-(1-y_i)^{\delta_2}\right] = 0, \tag{23}$$

and

$$\frac{\partial l^*}{\partial \delta_2} = \frac{n}{\delta_2} + \sum_{i=1}^{n}\log(1-y_i) - \sum_{i=1}^{n}\frac{(\delta_1-1)\log(1-y_i)}{\left[(1-y_i)^{-\delta_2}-1\right]} = 0. \tag{24}$$

Notably, there are no closed-form solutions for Equations (23 and 24). Therefore, in order to derive the ML estimators $\widehat{\delta}_1$ of δ_1 and $\widehat{\delta}_2$ of δ_2, numerical approaches using optim function in the R programming language are required. Furthermore, based on invariance property, the ML estimators of different entropy measures are produced after substituting $\widehat{\delta}_1$ and $\widehat{\delta}_2$ in Equations (16, 18, 20, and 22) to produce $\widehat{\chi}_1, \widehat{\chi}_2, \widehat{\chi}_3$ and $\widehat{\chi}_4$.

5.2 | Least Squares and Weighted Least Squares

In this sub-section, the LS and WLS estimators of the parameters are obtained. Let $y_{(1)} < y_{(2)} < \ldots < y_{(n)}$ represent the ordered observed sample of size n from the UIEP distribution. The LS and WLS estimators of unknown parameters of the UIEP distribution are obtained by minimizing the error of sum squares.

$$E^*(\delta_1,\delta_2) = \sum_{j=1}^{n}\upsilon_j\left[\left[1-(1-y_{(j)})^{\delta_2}\right]^{\delta_1} - \frac{j}{n+1}\right]^2.$$

The LS estimators $\overline{\delta}_1$ of δ_1 and $\overline{\delta}_2$ of δ_2 can be determined for $\upsilon_j = 1$. While the WLS estimators $\widehat{\delta}_1$ of $\delta_1$and $\widehat{\delta}_2$ of δ_2 can be determined for $\upsilon_j = \frac{(n+1)^2(n+2)}{j(n-j+1)}$. These estimates can also be obtained by solving the equations below using an iterative method:

$$\frac{\partial E^*(\delta_1,\delta_2)}{\partial \delta_1} = \sum_{j=1}^{n}\upsilon_j\left[\left[1-(1-y_{(j)})^{\delta_2}\right]^{\delta_1} - \frac{j}{n+1}\right]\vartheta_{\delta_1} = 0,$$

$$\frac{\partial E^*(\delta_1,\delta_2)}{\partial \delta_2} = \delta_1\sum_{j=1}^{n}\upsilon_j\left[\left[1-(1-y_{(j)})^{\delta_2}\right]^{\delta_1} - \frac{j}{n+1}\right]\vartheta_{\delta_2} = 0,$$

where

$$\vartheta_{\delta_1} = \left[1-(1-y_{(j)})^{\delta_2}\right]^{\delta_1}\log\left[1-(1-y_{(j)})^{\delta_2}\right],$$

$$\vartheta_{\delta_2} = -\delta_1\left[1-(1-y_{(j)})^{\delta_2}\right]^{\delta_1-1}(1-y_{(j)})^{\delta_2}\log(1-y_{(j)}). \tag{25}$$

Furthermore, the LS estimators of Ré, H−C, TS, and AR measures are produced, following the same procedure presented by Jha et al. [58], after substituting $\overline{\delta}_1$ and $\overline{\delta}_2$ in Equations (16, 18, 20, and 22) to produce $\overline{\chi}_1, \overline{\chi}_2, \overline{\chi}_3$ and $\overline{\chi}_4$. Similarly, Furthermore, the WLS estimators of Ré, H−C, TS, and AR measures are produced after substituting $\widehat{\delta}_1$ and $\widehat{\delta}_2$ in Equations (16, 18, 20, and 22) to produce $\widehat{\chi}_1, \widehat{\chi}_2, \widehat{\chi}_3$ and $\widehat{\chi}_4$.

5.3 | Anderson−Dalring & Kolmogorov

This subsection presents the AD estimation method for the parameters $\delta_1$and δ_2 of the UIEP distribution based on minimizing a goodness-of-fit statistic. This approach relies on comparing the estimated CDF to the empirical CDF of the observed data. Let $y_{(1)} < y_{(2)} < \ldots < y_{(n)}$ represent the ordered observed sample of size n from the UIEP distribution. The AD estimators of $\dddot{\delta}_1$ of δ_1 and $\dddot{\delta}_2$ of δ_2 are obtained by minimizing the following function

$$E_1^*(\delta_1,\delta_2) = -n - \frac{1}{n}\sum_{j=1}^{n}(2j-1)\left[\log\left(\left[1-\left(1-y_{(j)}\right)^{\delta_2}\right]^{\delta_1}\right) + \log\left(1-\left[1-\left(1-y_{(n-j+1)}\right)^{\delta_2}\right]^{\delta_1}\right)\right].$$

The following non-linear equations are solved using an iterative method implemented in R, yielding the AD estimators $\dddot{\delta}_1$ and $\dddot{\delta}_2$

$$\frac{\partial E_1^*(\delta_1,\delta_2)}{\partial \delta_1} = -\frac{1}{n}\sum_{j=1}^{n}(2j-1)\left[\frac{\vartheta_{\delta_1}}{\left[1-\left(1-y_{(j)}\right)^{\delta_2}\right]^{\delta_1}} - \frac{\vartheta_{\delta_1}}{1-\left[1-\left(1-y_{(j)}\right)^{\delta_2}\right]^{\delta_1}}\right] = 0,$$

$$\frac{\partial E_1^*(\delta_1,\delta_2)}{\partial \delta_2} = -\frac{1}{n}\sum_{j=1}^{n}(2j-1)\left[\frac{\vartheta_{\delta_2}}{\left[1-\left(1-y_{(j)}\right)^{\delta_2}\right]^{\delta_1}} - \frac{\vartheta_{\delta_2}}{1-\left[1-\left(1-y_{(j)}\right)^{\delta_2}\right]^{\delta_1}}\right] = 0,$$

where ϑ_{δ_1} and ϑ_{δ_2} are defined in Equation (25). Furthermore, the AD estimators of Ré, H−C, TS, and AR measures are produced after substituting $\dddot{\delta}_1$ and $\dddot{\delta}_2$ in Equations (16, 18, 20, and 22) to produce $\dddot{\chi}_1, \dddot{\chi}_2, \dddot{\chi}_3$ and $\dddot{\chi}_4$.

Finally, the parameters δ_1 and δ_2 of the UIEP distribution are determined using the KO method. Maximizing the following equation, with respect to the parameters δ_1 and δ_2 to produce the KO estimators' parameters $\ddot{\delta}_1$ and $\ddot{\delta}_2$ is the aim of the following estimating procedure:

$$E_2^*(\delta_1,\delta_2) = \underset{1\le j\le n}{Max}\sum_{j=1}^{n}\left[\frac{j}{n} - \left[1-\left(1-y_{(j)}\right)^{\delta_2}\right]^{\delta_1}, \left[1-\left(1-y_{(j)}\right)^{\delta_2}\right]^{\delta_1} - \frac{j-1}{n}\right].$$

Also, the KO estimators $\ddot{\chi}_1, \ddot{\chi}_2, \ddot{\chi}_3$ and $\ddot{\chi}_4$ are produced after inserting $\ddot{\delta}_1$ and $\ddot{\delta}_2$ in Equations (16, 18, 20, and 22).

6 | Numerical Simulation

A simulation study was conducted to evaluate the effectiveness of multiple estimation strategies for Ré, H−C, TS, and AR entropy measures and parameters δ_1, δ_2 in UIEP distribution. The study considered sample sizes n of 25, 50, 75, 100, and 200, with $N = 1000$ replication numbers. Specifically, the UIEP distribution was constructed by choosing the following parameter values as

- The true values on Table A1 are set1 = ($\delta_1 = 0.5, \delta_2 = 1.4, b = 0.9$), while the corresponding true values of entropy measures are Ré = −0.40489, H−C = −0.55285, TS = −0.39680, and AR = −0.39592.
- The true values on Table A2 are set 2 = ($\delta_1 = 2, \delta_2 = 0.6, b = 0.9$), white the associated true values of entropy measures are Ré = −0.61617, H−C = −0.83257, TS = −0.59757, and AR = −0.59555.
- The true values on Table A3 are set 3 = ($\delta_1 = 0.8, \delta_2 = 2, b = 1.5$), while the associated true values of entropy measures are Ré = −0.38956, H−C = −0.73420, TS = −0.43008, and AR = −0.41598.
- The true values Table A4. are set 4 = ($\delta_1 = 2.2, \delta_2 = 0.8, b = 1.5$), while the associated true values of entropy measures are Ré = −0.54937, H−C = −1.07929, TS = −0.63223, and AR = −0.60289.

were carefully selected to ensure a wide range of entropy levels. Furthermore, this study employed four distinct entropy measures: Ré, TS, AR, and H−C. Five estimating approaches: ML, KO, LS, WLS, and AD were examined. Uniform random numbers between 0 and 1 were created, and sample size n of the UIEP distribution was obtained with the QF. The performance of entropy measures and parameters has been evaluated using absolute biases (ABs) and mean squared errors (MSEs).

All simulations were implemented in the R programming language, employing the "optim" function for estimation. The findings are summarized in Tables A1−A4 (see Appendix A) and Figures 5 and 6.

- As n increases, the ABs and MSEs of each estimate decrease.
- The KO method is the most efficient compared to all other estimation methods for the parameters of the UIEP distribution.
- As true values of δ_1 and δ_2 increase, the estimates for δ_1 and δ_2 generally show an increase in MSE across all methods.
- At $b = 1.5$, under the LS method, when δ_1 is less than δ_2, the H−C entropy estimates show a higher increase in MSE than the TS entropy estimates. However, when δ_2 is less than δ_1, the TS entropy estimate shows a higher increase in MSE than the H−C entropy estimate.
- At $b = 0.9$, the AR entropy estimation is the best compared to all other entropy estimation methods for the UIEP distribution.
- At $b = 1.5$, the Ré entropy estimation is the best compared to all other entropy estimation methods for the UIEP distribution.
- Both the AR and Ré entropy estimators are found to be best when using ML estimation. The AR estimate is preferred for low-entropy order value, whereas Ré is the superior choice for high-entropy order value.

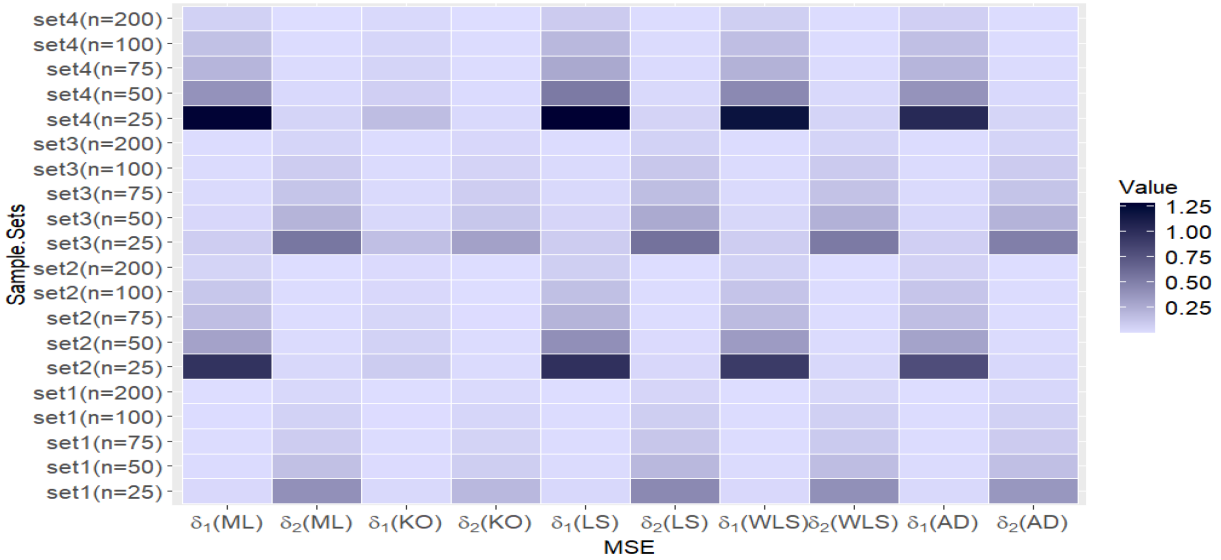

FIGURE 5 | Heatmaps of MSE values for parameters of the UIEP distribution with different methods.

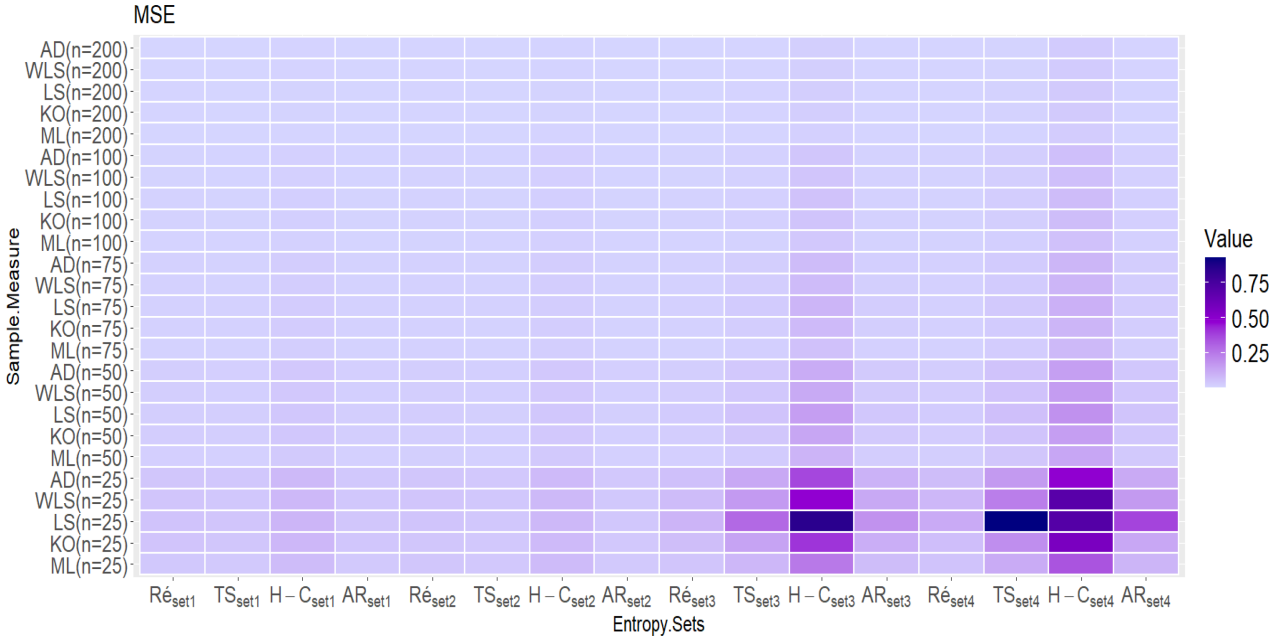

FIGURE 6 | Heatmaps of MSE values for entropy measures of the UIEP distribution with different methods.

7 | Real Data Application

This section investigates the UIEP distribution by comparing it to well-known unit distributions available in the literature. For this comparison, two datasets are used: one with coronavirus data and one with rock samples from a petroleum reserve. The following distributions are examined for comparison: UEP distribution, UEL distribution, UEHL distribution, KW distribution, ETL distribution (Pourdarvish et al. [59]), ULL distribution, and UPL distribution.

The ML method was employed to parameterize competing distributions. The KO, LS, WLS, and AD techniques are used to estimate the parameters for the UIEP distribution. The model selection process used the log-likelihood-derived are the Akaike information criterion (λ_1), Bayesian information criterion (λ_2), consistent Akaike information criterion (λ_3), Hannan–Quinn information criterion (λ_4). The AD statistic (λ_5), the Cramér–von Mises statistic (λ_6), the Kolmogorov–Smirnov statistic (λ_7), and the p-value (λ_8) were used to evaluate goodness-of-fit. Superior fit is indicated by lower λ_1, λ_2, λ_3, λ_4, λ_5, λ_6, and λ_7 values as well as a higher λ_8. This method compares UIEP with other distributions provided. All cods are given in Appendix B.

i. COVID Data

For an 82-day period in 2021, from May 1 to July 16, COVID-19 death rates were recorded in England (see Abu El Azm et al. [60]). The data are as follows: 0.0023, 0.0023, 0.0023, 0.0046, 0.0065,

0.0067, 0.0069, 0.0069, 0.0091, 0.0093, 0.0093, 0.0093, 0.0111, 0.0115, 0.0116, 0.0116, 0.0119, 0.0133, 0.0136, 0.0138, 0.0138, 0.0159, 0.0161, 0.0162, 0.0162, 0.0162, 0.0163, 0.0180, 0.0187, 0.0202, 0.0207, 0.0208, 0.0225, 0.0230, 0.0230, 0.0239, 0.0245, 0.0251, 0.0255, 0.0255, 0.0271, 0.0275, 0.0295, 0.0297, 0.0300, 0.0302, 0.0312, 0.0314, 0.0326, 0.0346, 0.0349, 0.0350, 0.0355, 0.0379, 0.0384, 0.0394, 0.0394, 0.0412, 0.0419, 0.0425, 0.0461, 0.0464, 0.0468, 0.0471, 0.0495, 0.0501, 0.0521, 0.0571, 0.0588, 0.0597, 0.0628, 0.0679, 0.0685, 0.0715, 0.0766, 0.0780, 0.0942, 0.0960, 0.0988, 0.1223, 0.1343, and 0.1781.

The COVID-19 data's key descriptive statistics are tabulated in Table 2 and visualized in Figure 7.

Figure 7 examines the total test time (TTT) plot and its relationship to HRF, demonstrating an excellent fit with the UIEP distribution. The PDF analysis shows asymmetrical data distribution. Quantile–quantile (QQ) and box plots are used to test normality and observe outliers, with the mean in red and outliers shown by blue rings on the plots. The left-hand panel of Table 3 shows the results of KO, LS, WLS, and AD estimation, along with their associated SEs, calculated specifically for the UIEP distribution. The right-hand panel of Table 3 presents the results of the ML estimation, including standard errors (SEs), for all distributions. Figure 8 illustrates a comparison of the SEs of different estimates for the UIEP distribution.

Table 4 and Figure 8 collectively indicate that the KO method offers the most reliable estimates, validating the simulation outcomes for the UIEP distribution. The goodness of fit measures as λ_1, λ_2, λ_3, λ_4, λ_5, λ_6, λ_7, and λ_8 for the COVID-19 data are also shown in Table 4.

Figures 9–11 assess the UIEP distribution's fit to the COVID-19 data. Figure 9 shows the log-likelihood curve parameters for the UIEP distribution, which proves the estimators' maximizing. Figure 10 compares the estimated and empirical CDFs and the estimated PDFs with a histogram. Figure 11 displays a P–P plot of the UIEP distribution demonstrating the model's sufficiency.

ii. Petroleum Reservoir Data

There are 48 rock samples in the dataset, all taken from a petroleum reservoir discussed by Cordeiro and Brito [61]. The values for these samples are 0.0903296, 0.2036540, 0.2043140, 0.2808870, 0.1976530, 0.3286410, 0.1486220, 0.1623940, 0.2627270, 0.1794550, 0.3266350, 0.2300810, 0.1833120, 0.1509440, 0.2000710, 0.1918020, 0.1541920, 0.4641250, 0.1170630, 0.1481410, 0.1448100, 0.1330830, 0.2760160, 0.4204770, 0.1224170, 0.2285950, 0.1138520, 0.2252140, 0.1769690, 0.2007440, 0.1670450, 0.2316230, 0.2910290, 0.3412730, 0.4387120, 0.2626510, 0.1896510, 0.1725670,

TABLE 2 | Summary statistics for COVID-19 data.

Minimum	Q_1	Q_2	μ_1'	Q_3	Maximum	σ^2	SK	KU
0.002	0.014	0.027	0.036	0.046	0.178	0.001	2.021	8.176

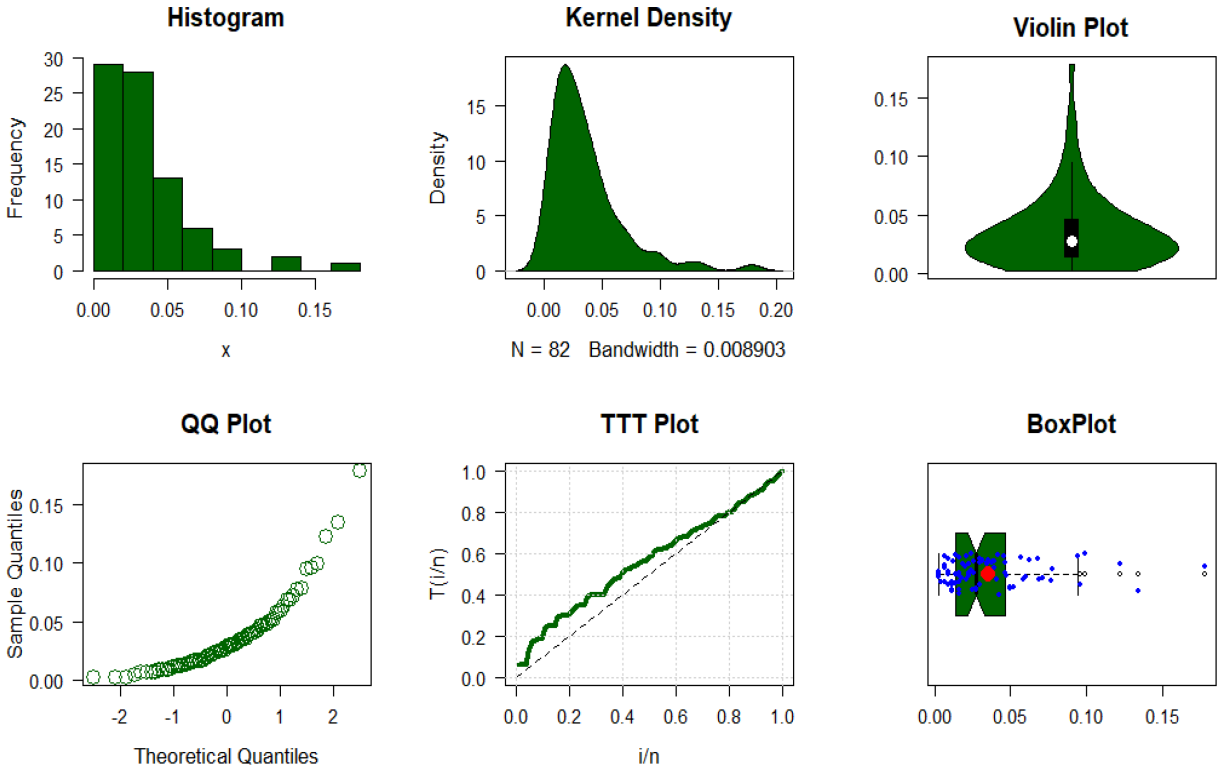

FIGURE 7 | Descriptive visualizations of COVID-19 data.

TABLE 3 | The estimates associated with the SEs derived from different distributions for COVID-19 data.

Distribution	UIEP					UEP	UEL	UEHL	UG	ETL	ULL	UPL
Methods	**ML**	**KO**	**LS**	**WLS**	**AD**				**ML**			
$\hat{\delta}_1$	1.604	0.203	1.484	1.611	1.622	1.186	0.033	29.313	55.316	1.256	7.195	4.120
$\hat{\delta}_2$	36.161	1.139	35.381	37.499	37.613	0.087	41.763	1.251	1.238	24.979	3.597	1.868
$\hat{\delta}_3$	—	—	—	—	—	2.462	71.919	—	—	—	—	356.314
SE $(\hat{\delta}_1)$	0.257	0.026	1.222	0.054	0.481	0.096	0.016	9.285	18.084	0.111	0.662	0.383
SE $(\hat{\delta}_2)$	4.725	0.111	23.935	1.023	8.819	0.343	18.526	0.103	0.105	6.944	0.096	0.665
SE $(\hat{\delta}_3)$	—	—	—	—	—	11.530	26.624	—	—	—	—	115.113

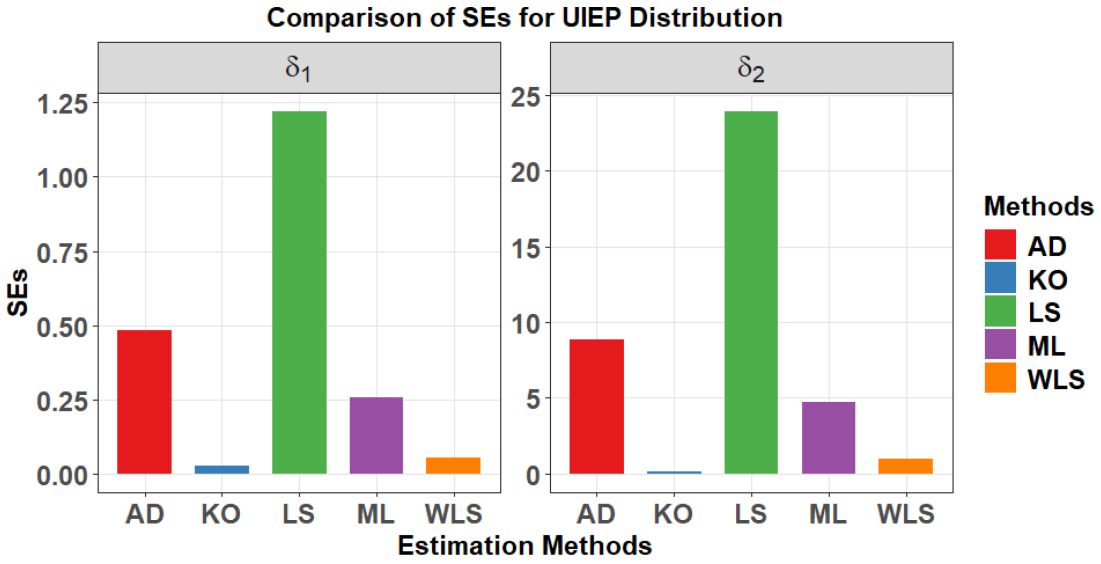

FIGURE 8 | Comparison of SEs for the UIEP distribution across COVID-19 data.

TABLE 4 | Measurements of goodness of fit for COVID-19 data.

Name	UIEP	UEP	UEL	UEHL	KW	ETL	ULL	UPL
λ_1	−387.304	−369.451	−381.515	−385.054	−384.669	−384.877	−387.076	−370.001
λ_2	−382.491	−362.231	−374.295	−380.241	−379.856	−380.063	−382.063	−362.781
λ_3	−387.152	−369.143	−381.208	−384.902	−384.517	−384.725	−387.025	−369.693
λ_4	−385.372	−366.552	−378.617	−383.122	−382.737	−382.944	−385.144	−367.102
λ_5	0.032	0.071	0.074	0.055	0.060	0.058	0.079	0.012
λ_6	0.244	0.494	0.509	0.393	0.421	0.411	0.749	0.109
λ_7	0.053	0.064	0.063	0.058	0.060	0.059	0.054	0.963
λ_8	0.974	0.886	0.901	0.949	0.931	0.938	0.969	0.054

0.2400770, 0.3116460, 0.1635860, 0.1824530, 0.1641270, 0.1534810, 0.1618650, 0.2760160, 0.2538320, and 0.2004470.

The petroleum reservoir data's key descriptive statistics are tabulated in Table 5 and visualized in Figure 12.

Following a summary of the petroleum reservoir data, Figure 12 examines the TTT plot and its relationship to HRF, demonstrating an excellent fit with the UIEP distribution. The PDF analysis shows asymmetrical data distribution. QQ and box plots are used to test normality and observe outliers, with the mean in red and outliers shown by blue rings on the plots. Table 6 displays the results of ML, KO, LS, WLS, and AD estimation, along with their associated SEs Figure 13 shows a comparison of the SEs of estimation methods for the UIEP distribution.

Analysis of Table 6 and Figure 13 demonstrates that the KO method provides the most accurate estimation, corroborating the

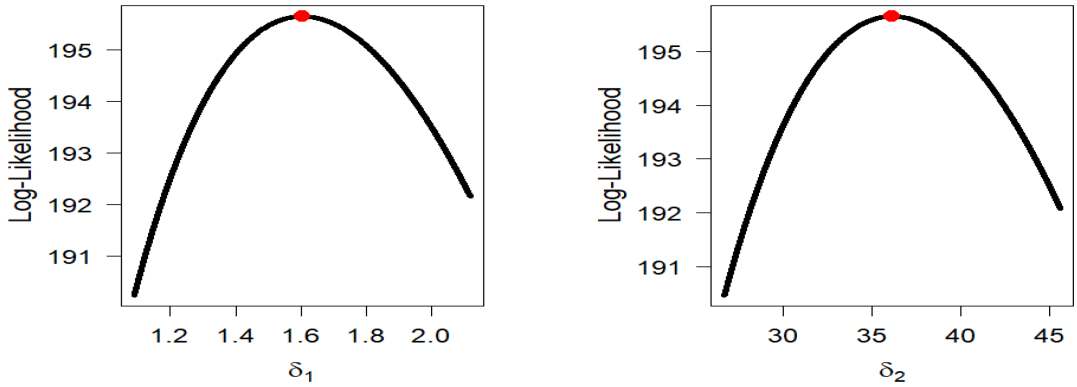

FIGURE 9 | Profile-Log-likelihood for parameters δ_1 and δ_2 of COVID-19 data.

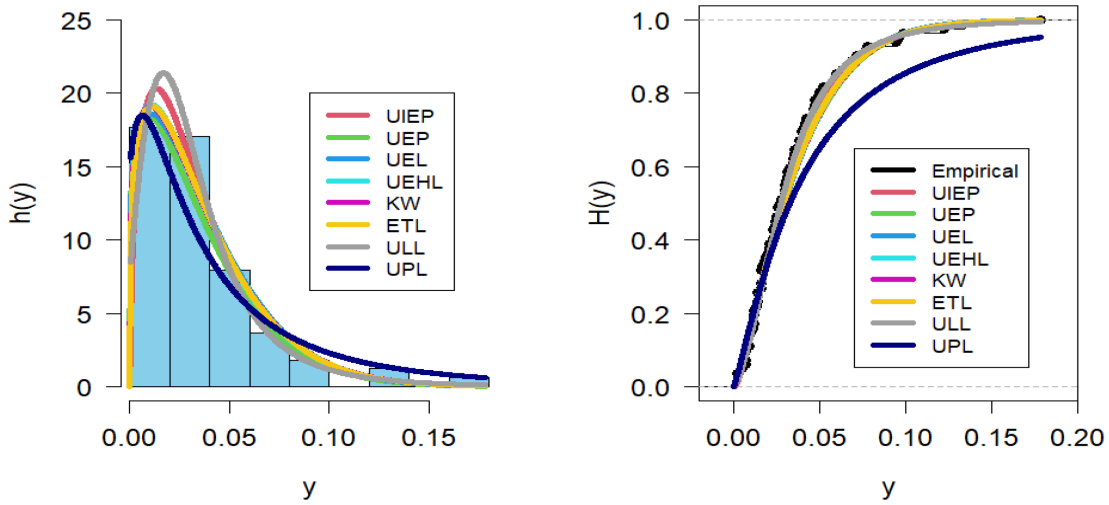

FIGURE 10 | PDF and CDF estimates for the COVID-19 data.

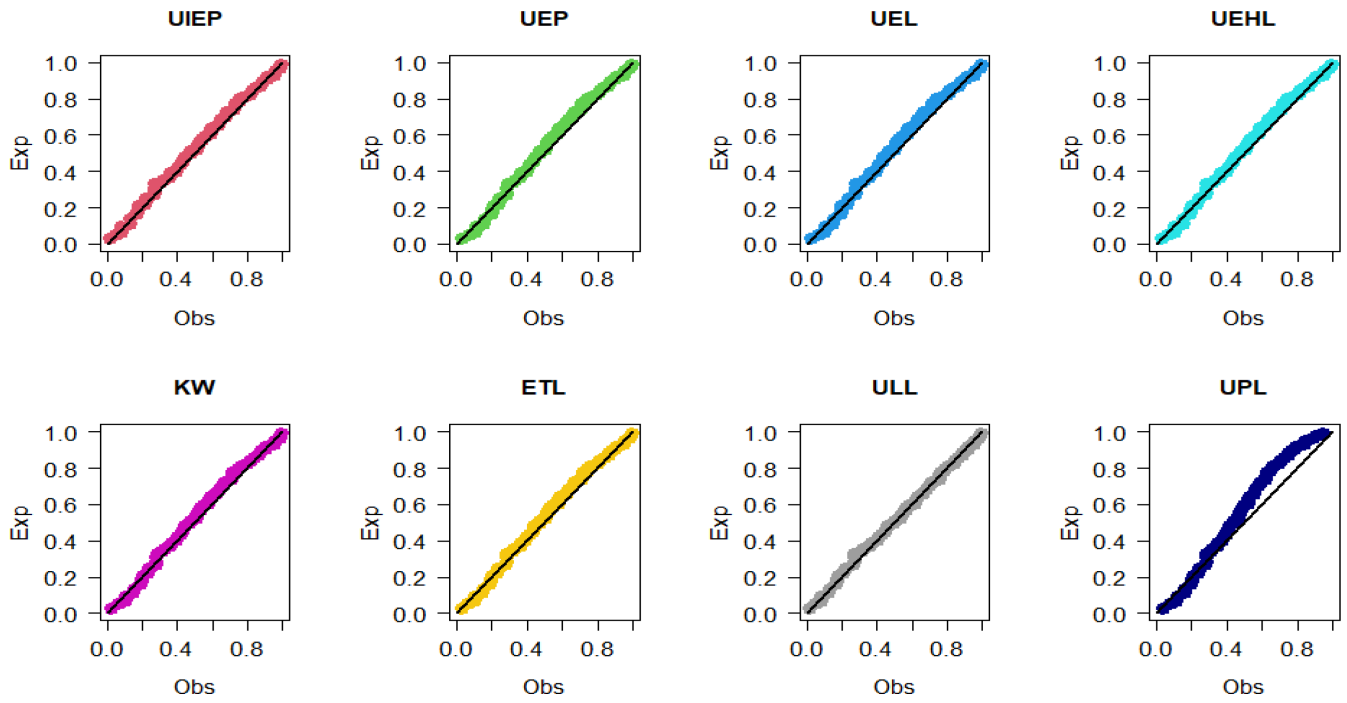

FIGURE 11 | PP plots for different distributions of COVID-19 data.

TABLE 5 | Summary statistics for petroleum reservoir data.

Minimum	Q_1	Q_2	μ_1'	Q_3	Maximum	σ^2	SK	KU
0.090	0.162	0.199	0.218	0.263	0.464	0.007	1.169	4.110

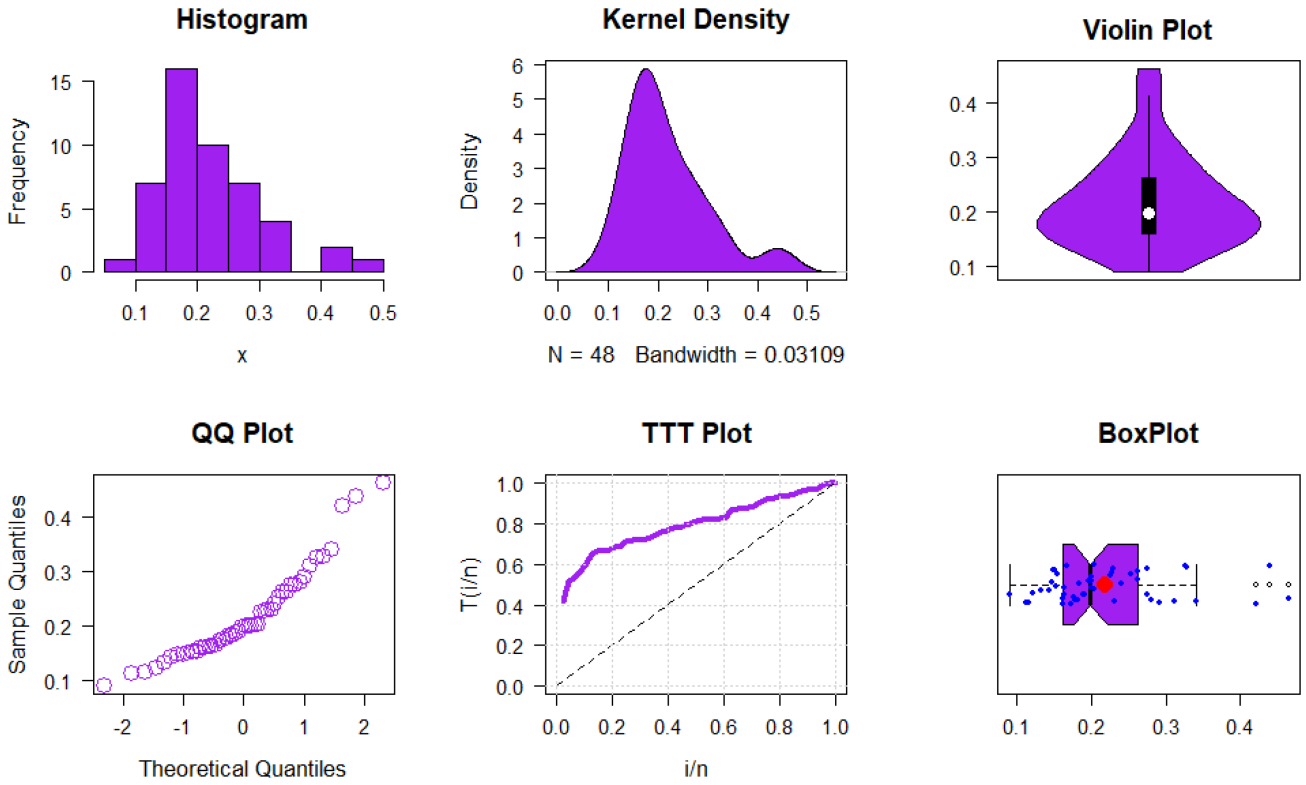

FIGURE 12 | Descriptive visualizations of petroleum reservoir data.

TABLE 6 | The estimates associated with the SEs derived from the distribution of petroleum reservoir data.

Distribution	UIEP					UEP	UEL	UEHL	UG	ETL	ULL	UPL
Methods	ML	KO	LS	WLS	AD				ML			
$\hat{\delta}_1$	11.564	0.854	10.847	10.908	10.905	1.968	0.045	23.694	44.440	3.136	7.404	5.644
$\hat{\delta}_2$	12.285	2.291	12.373	12.267	12.235	0.298	63.783	2.746	2.715	13.641	1.582	4.164
$\hat{\delta}_3$	—	—	—	—	—	0.792	49.538	—	—	—	—	74.019
SE $(\hat{\delta}_1)$	3.891	0.065	21.015	1.058	7.149	0.199	0.035	8.954	17.444	0.364	0.898	0.870
SE $(\hat{\delta}_2)$	1.625	0.115	8.936	0.461	2.990	2.942	45.985	0.285	0.293	4.199	0.053	3.389
SE $(\hat{\delta}_3)$	—	—	—	—	—	15.365	20.603	—	—	—	—	52.583

simulation results for the UIEP distribution. The goodness of fit measures as λ_1, λ_2, λ_3, λ_4, λ_5, λ_6, λ_7, and λ_8 for the petroleum reservoir data are also shown in Table 7.

Figures 14–16 assess the UIEP distribution's fit to the COVID-19 data. Figure 14 shows the log-likelihood curve parameters for the UIEP distribution, which proves the estimators' maximizing. Figure 15 compares the estimated and empirical CDFs and the estimated PDFs with a histogram. Figure 16 displays a P–P plot of the UIEP distribution demonstrating the model's sufficiency.

8 | Concluding Remarks

Unit distributions serve a key role in statistical modeling and are essential for assessing variables that are restricted to the interval [0,1]. In this study, we present the UIEP distribution, a new two-parameter model. Numerous forms are displayed by the UIEP, such as rising, J-shaped, or U-shaped hazard rate functions, as well as unimodal, reversed J-shaped, left-skewed, and right-skewed density functions. Its applicability for modeling unit data is improved by this flexibility. Quantiles, moments,

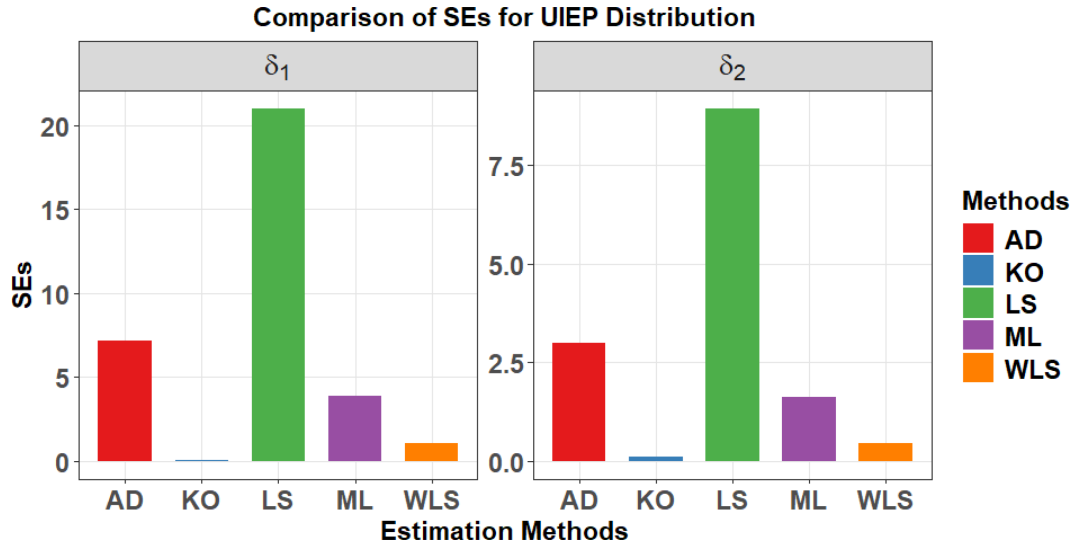

FIGURE 13 | Comparison of SEs for the UIEP distribution across petroleum reservoir data.

TABLE 7 | Measurements of goodness of fit for petroleum reservoir data.

Name	UIEP	UEP	UEL	UEHL	UG	ETL	ULL	UPL
λ_1	−110.825	−45.004	−98.266	−101.451	−100.983	−102.712	−106.497	−110.169
λ_2	−107.083	−39.391	−92.653	−97.709	−97.241	−98.969	−102.755	−104.555
λ_3	−110.559	−44.459	−97.721	−101.184	−100.716	−102.445	−106.230	−109.623
λ_4	−109.411	−42.883	−96.145	−100.037	−99.569	−101.298	−105.083	−108.047
λ_5	0.072	0.281	0.218	0.201	0.208	0.187	0.127	0.096
λ_6	0.428	1.737	1.337	1.230	1.279	1.142	0.748	0.731
λ_7	0.117	0.159	0.154	0.150	0.153	0.153	0.212	0.389
λ_8	0.524	0.177	0.206	0.229	0.210	0.215	0.487	0.370

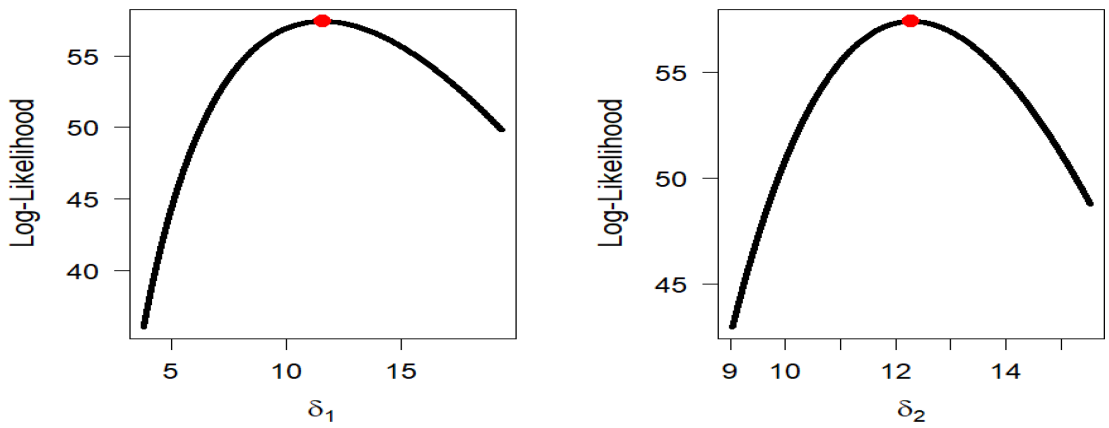

FIGURE 14 | Profile-Log-likelihood for parameters δ_1 and δ_2 of for petroleum reservoir data.

PWM, SO, important uncertainty measures, Lorenz and Bonferroni curves, and the S-SR parameter are among the important statistical features that we derive analytically. To estimate distribution parameters and evaluate entropy measures, the statistical analysis uses a number of estimation approaches, such as ML, WLS, AD, LS, and KO. According to simulation data, the KO technique is the most successful estimation strategy among those studied for the parameters and entropy measures of the UIEP distribution. For lower entropy orders, the AR entropy typically performs better under ML estimation, whereas Ré entropy works better for higher entropy orders. This observation highlights a clear relationship between the entropy order and the optimal estimator. In order to verify the suggested distribution, we apply it to two real-world datasets: geological data from petroleum rock

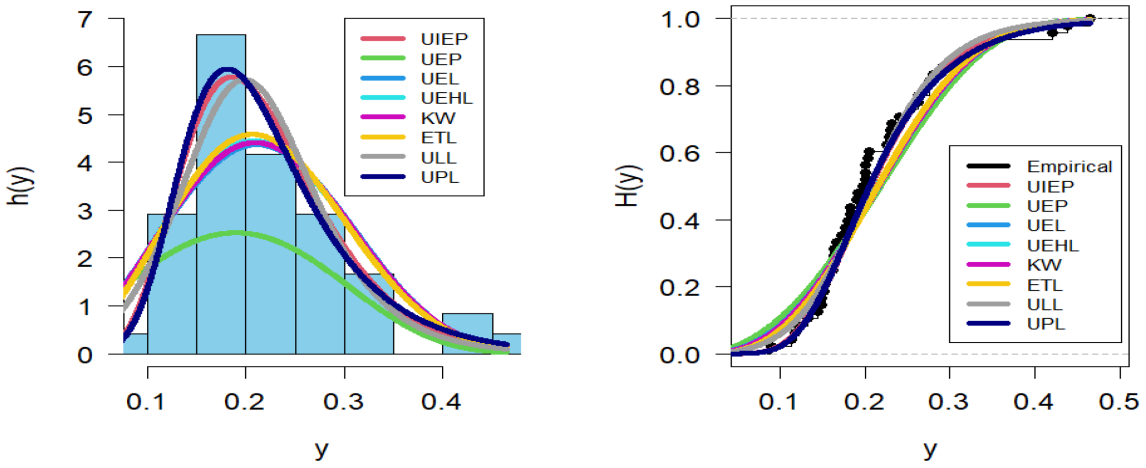

FIGURE 15 | PDF and CDF estimates for petroleum reservoir data.

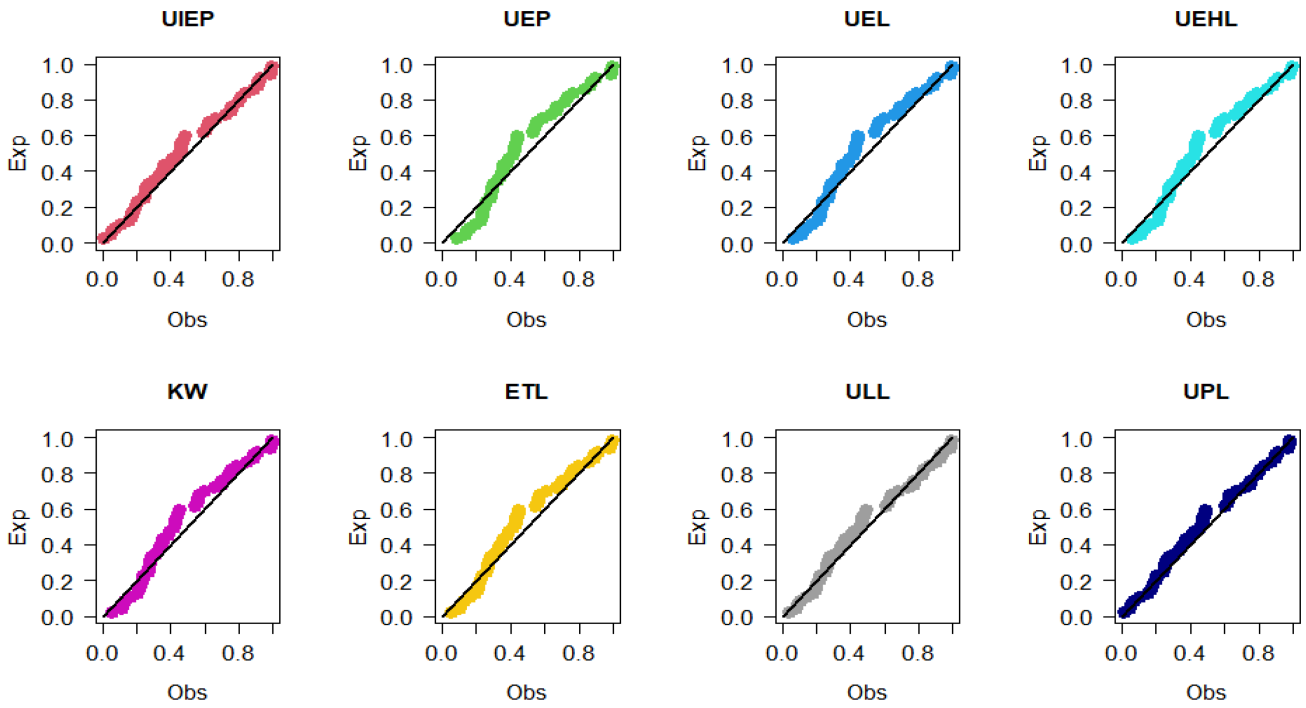

FIGURE 16 | PP plots for different distributions of petroleum reservoir data.

samples and health data associated with COVID-19. The model fit of these applications is better than that of other distributions. This study, although useful, has one drawback that should be noted. Primarily, this study utilizes four traditional estimation techniques along with large sample sizes. These methods are sensitive to small sample sizes, which can produce fewer stable estimates. The reliability of our conclusions may be impacted when working with smaller datasets, as this could result in less stable estimates or potentially prevent the model from converging. Future research could significantly benefit from exploring Bayesian estimation techniques. This approach is advantageous, especially when dealing with smaller samples, because it allows the use of informative priors and hierarchical modeling. Furthermore, implementing the UIEP distribution on real-world datasets with more complex structures would be essential in further verifying its practical usefulness.

Author Contributions

Amal S. Hassan: conceptualization, writing – original draft, writing – review and editing, methodology. **Gaber Sallam Salem Abdalla:** writing – original draft, writing – review and editing, conceptualization. **Abdoulie Faal:** writing – original draft, writing – review and editing, methodology. **Omar A. Saudi:** conceptualization, methodology, software, formal analysis, writing – original draft.

Acknowledgments

This work was supported and funded by the Deanship of Scientific Research at Imam Mohammad Ibn Saud Islamic University (IMSIU) (grant number IMSIU-DDRSP2501).

Conflicts of Interest

The authors declare no conflicts of interest.

Data Availability Statement

The data that support the findings of this study are available on request from the corresponding author. The data are not publicly available due to privacy or ethical restrictions.

References

1. V. K. Sharma, S. K. Singh, U. Singh, and V. Agiwal, "The Inverse Lindley Distribution: A Stress-Strength Reliability Model With Application to Head and Neck Cancer Data," *Journal of Industrial and Production Engineering* 32, no. 3 (2015): 162–173.

2. K. V. P. Barco, J. Mazucheli, and V. Janeiro, "The Inverse Power Lindley Distribution," *Communications in Statistics - Simulation and Computation* 46, no. 8 (2017): 6308–6323.

3. S. Lee, Y. Noh, and Y. Chung, "Inverted Exponentiated Weibull Distribution With Applications to Lifetime Data," *Communications for Statistical Applications and Methods* 24, no. 3 (2017): 227–240.

4. F. Louzada, P. L. Ramos, and D. Nascimento, "The Inverse Nakagami-m Distribution: A Novel Approach in Reliability," *IEEE Transactions on Reliability* 67, no. 3 (2018): 1030–1042.

5. A. M. Abd AL-Fattah, A. A. El-Helbawy, and G. R. Al-Dayian, "Inverted Kumumaraswamy Distribution: Properties and Estimation," *Pakistan Journal of Statistics* 33, no. 1 (2017): 37–61.

6. A. S. Hassan and M. Abd-Allah, "On the Inverse Power Lomax Distribution," *Annals of Data Science* 6, no. 2 (2019): 259–278.

7. M. H. Tahir, G. M. Cordeiro, S. Ali, S. Dey, and A. Manzoor, "The Inverted Nadarajah–Haghighi Distribution: Estimation Methods and Applications," *Journal of Statistical Computation and Simulation* 88, no. 14 (2018): 2775–2798.

8. A. S. Hassan and R. E. Mohammed, "Parameter Estimation of Inverse Exponentiated Lomax Distribution With Right Censored Data," *Gazi University Journal of Science* 32, no. 4 (2019): 1370–1386.

9. A. S. Yadav, S. S. Maiti, and M. Saha, "The Inverse Xgamma Distribution: Statistical Properties and Different Methods of Estimation," *Annals of Data Science* 8, no. 2 (2021): 275–293, https://doi.org/10.1007/s40745-019-00211-w.

10. A. S. Hassan and S. G. Nassr, "The Inverse Weibull Generator of Distributions: Properties and Applications," *Journal of Data Science* 16, no. 4 (2018): 732–742, https://doi.org/10.6339/JDS.201810_16(4).00004.

11. Y. Y. Abdelall, A. S. Hassan, and E. M. Almetwally, "A New Extension of the Odd Inverse Weibull-G Family of Distributions: Bayesian and Non-Bayesian Estimation With Engineering Applications," *Computational Journal of Mathematical and Statistical Sciences* 3, no. 2 (2024): 359–388, https://doi.org/10.21608/CJMSS.2024.285399.1050.

12. M. H. Omar, S. Y. Arafat, M. P. Hossain, and M. Riaz, "Inverse Maxwell Distribution and Statistical Process Control: An Efficient Approach for Monitoring Positively Skewed Process," *Symmetry* 13, no. 2 (2021): 189.

13. A. S. Hassan, M. Elgarhy, and R. Ragab, "Statistical Properties and Estimation of Inverted Topp-Leone Distribution," *Journal of Statistical Applications & Probability* 9, no. 2 (2020): 319–331.

14. S. Dankunprasert, U. Jaroengeratikun, and T. Talangtam, "The Properties of Inverse Pareto Distribution and Its Application to Extreme Events," *Thailand Statistician* 19, no. 1 (2021): 1–13.

15. K. K. Shukla, "Inverse Ishita Distribution: Properties and Applications," *Reliability Theory and Applications* 16, no. 1 (2021): 98–108.

16. M. M. Al Sobhi, "The Inverse-Power Logistic-Exponential Distribution: Properties, Estimation Methods, and Application to Insurance Data," *Mathematics* 8, no. 11 (2020): 2060.

17. L. P. Sapkota and V. Kumar, "Applications and Some Characteristics of Inverse Power Cauchy Distribution," *Reliability: Theory & Applications* 18, no. 1 (2023): 301–315.

18. A. Al Mutairi, A. S. Hassan, S. S. Alshqaq, et al., "Inverse Power Ramos-Louzada Distribution With Various Classical Estimation Methods and Modeling to Engineering Data," *AIP Advances* 13, no. 9 (2023): 095117, https://doi.org/10.1063/5.0170393.

19. J. Chisimkwuo, M. P. Tal, P. T. Pokalas, and J. Ohakwe, "Inverse Shanker Distribution: Its Properties and Application," *African Journal of Mathematics and Statistics Studies* 7, no. 3 (2024): 29–42, https://doi.org/10.52589/AJMSS-JRADHTY.

20. A. S. Hassan, O. A. Saudi, and H. F. Nagy, "A New Three-Parameter Inverted Exponentiated Weibull Distribution: Statistical Inference and Application," *Egyptian Statistical Journal* 68, no. 2 (2024): 34–64.

21. I. Elbatal, A. S. Hassan, A. M. Gemeay, L. S. Diab, A. B. Ghorbal, and M. Elgarhy, "Statistical Analysis of the Inverse Power Zeghdoudi Model: Estimation, Simulation and Modeling to Engineering and Environmental Data," *Physica Scripta* 99, no. 6 (2024): 065231, https://doi.org/10.1088/1402-4896/ad46d0.

22. T. Z. Sindhu, A. Shafiq, M. B. Riaz, et al., "Introducing the New Arcsine-Generator Distribution Family: An In-Depth Exploration With an Illustrative Example of the Inverse Weibull Distribution for Analyzing Healthcare Industry Data," *Journal of Radiation Research and Applied Sciences* 17, no. 2 (2024): 100879, https://doi.org/10.1016/j.jrras.2024.100879.

23. M. E. Ghitany, V. K. Tuan, and N. Balakrishnan, "Likelihood Estimation for a General Class of Inverse Exponentiated Distributions Based on Complete and Progressively Censored Data," *Journal of Statistical Computation and Simulation* 84, no. 1 (2014): 96–106.

24. R. C. Gupta, R. D. Gupta, and P. L. Gupta, "Modeling Failure Time Data by Lehman Alternatives," *Communications in Statistics - Theory and Methods* 27, no. 4 (1998): 887–904.

25. B. Pradhan and D. Kundu, "On Progressively Censored Generalized Exponential Distribution," *Test* 18, no. 3 (2009): 497–515.

26. R. K. Maurya, Y. M. Tripathi, T. Sen, and M. K. Rastogi, "Inference for an Inverted Exponentiated Pareto Distribution Under Progressive Censoring," *Journal of Statistical Theory and Practice* 13 (2019): 2, https://doi.org/10.1007/s42519-018-0002-y.

27. F. F. Shaikh and M. N. Patel, "Inference for Inverted Exponentiated Pareto Distribution Based on Upper Record Values," *Revista Investigación Operacional* 43, no. 2 (2022): 192–202.

28. R. Kumari, Y. M. Tripathi, R. K. Sinha, and L. Wang, "Reliability Estimation for the Inverted Exponentiated Pareto Distribution," *Quality Technology & Quantitative Management* 20, no. 4 (2023): 485–510, https://doi.org/10.1080/16843703.2022.2125762.

29. A. Fayomi, A. S. Hassan, and E. A. Almetwally, "Reliability Inference for Multicomponent Systems Based on the Inverted Exponentiated Pareto Distribution and Progressive First Failure Censoring," *Journal of Nonlinear Mathematical Physics* 32, no. 12 (2025): 1–37, https://doi.org/10.1007/s44198-024-00262-5.

30. J. Mazucheli, A. F. B. Menezes, and S. Chakraborty, "On the One Parameter Unit-Lindley Distribution and Its Associated Regression Model for Proportion Data," *Journal of Applied Statistics* 46, no. 4 (2019): 700–714.

31. J. Mazucheli, A. F. Menezes, and S. Dey, "Unit-Gompertz Distribution With Applications," *Statistica* 79, no. 1 (2019): 25–43.

32. T. Z. Sindhu, A. Shafiq, J. Mazucheli, G. Ozel, and B. Alves, "Some Additional Facts About Unit-Gompertz Distribution," *Chilean Journal of Statistics* 14, no. 2 (2023): 143–171, https://doi.org/10.32372/ChJS.14-02-05.

33. J. Mazucheli, A. F. B. Menezes, L. B. Fernandes, R. P. De Oliveira, and M. E. Ghitany, "The Unit-Weibull Distribution as an Alternative to the Kumaraswamy Distribution for the Modeling of Quantiles Conditional on Covariates," *Journal of Applied Statistics* 47, no. 6 (2020): 954–974.

34. A. S. Hassan, A. Fayomi, A. Algarni, and E. M. Almetwally, "Bayesian and Non-Bayesian Inference for Unit-Exponentiated Half-Logistic Distribution With Data Analysis," *Applied Sciences* 12, no. 21 (2022): 11253, https://doi.org/10.3390/app122111253.

35. M. A. u. Haq, S. Hashmi, K. Aidi, P. L. Ramos, and F. Louzada, "Unit Modified Burr-III Distribution: Estimation, Characterizations and Validation Test," *Annals of Data Science* 10 (2023): 415–440, https://doi.org/10.1007/s40745-020-00298-6.

36. A. Fayomi, A. S. Hassan, and E. M. Almetwally, "Inference and Quantile Regression for the Unit-Exponentiated Lomax Distribution," *PLoS One* 18, no. 7 (2023): e0288635, https://doi.org/10.1371/journal.pone.0288635.

37. M. Ç. Korkmaz, "The Unit Generalized Half Normal Distribution: A New Bounded Distribution With Inference and Application," *UPB Scientific Bulletin, Series A: Applied Mathematics and Physics* 82, no. 2 (2020): 133–140.

38. L. D. Ribeiro-Reis, "Unit Log-Logistic Distribution and Unit Log-Logistic Regression Model," *Journal of the Indian Society for Probability and Statistics* 22, no. 2 (2021): 375–388.

39. G. Martínez-Flórez, R. B. Azevedo-Farias, and R. Tovar-Falón, "New Class of Unit-Power Skew-Normal Distribution and Its Associated Regression Model for Bounded Responses," *Mathematics* 10, no. 17 (2022): 3035.

40. A. S. Hassan and R. S. Alharbi, "Different Estimation Methods for the Unit Inverse Exponentiated Weibull Distribution," *Communications for Statistical Applications and Methods* 30, no. 2 (2023): 191–213.

41. M. Ç. Korkmaz and C. Chesneau, "On the Unit Burr-XII Distribution With the Quantile Regression Modeling and Applications," *Computational and Applied Mathematics* 40, no. 1 (2021): 29, https://doi.org/10.1007/s40314-021-01418-5.

42. A. Fayomi, A. S. Hassan, H. Baaqeel, and E. M. Almetwally, "Bayesian Inference and Data Analysis of the Unit-Power Burr X Distribution," *Axioms* 12, no. 3 (2023): 297, https://doi.org/10.3390/axioms12030297.

43. A. T. Ramadan, A. H. Tolba, and B. S. El-Desouky, "A Unit Half-Logistic Geometric Distribution and Its Application in Insurance," *Axioms* 11, no. 12 (2022): 676, https://doi.org/10.3390/axioms11120676.

44. S. Hashmi, M. Ahsan-ul-Haq, J. Zafar, and M. A. Khaleel, "Unit Xgamma Distribution: Its Properties, Estimation and Application: Unit-Xgamma Distribution," *Proceedings of the Pakistan Academy of Sciences. A, Physical and Computational Sciences* 59, no. 1 (2022): 15–28.

45. A. S. Hassan, A. M. Khalil, and H. F. Nagy, "Data Analysis and Classical Estimation Methods of the Bounded Power Lomax Distribution," *Reliability Theory & Applications* 19, no. 1 (2024): 770–789, https://doi.org/10.24412/1932-2321-2024-177-770-789.

46. A. Krishna, R. Maya, C. Chesneau, and M. R. Irshad, "The Unit Teissier Distribution and Its Applications," *Mathematical and Computational Applications* 27, no. 1 (2022): 12, https://doi.org/10.3390/mca27010012.

47. S. A. Lone, T. N. Sindhu, S. Anwar, M. K. H. Hassan, S. A. Alsahli, and T. A. Abushal, "On Construction and Estimation of Mixture of Log-Bilal Distributions," *Axioms* 12, no. 3 (2023): 309, https://doi.org/10.3390/axioms12030309.

48. T. N. Sindhu, A. Shafiq, and Z. Hussain, "Generalized Exponentiated Unit Gompertz Distribution for Modeling Arthritic Pain Relief Times Data: Classical Approach to Statistical Inference," *Journal of Biopharmaceutical Statistics* 34, no. 3 (2024): 323–348, https://doi.org/10.1080/10543406.2023.2210681.

49. A. Shafiq, T. N. Sindhu, Z. Hussain, J. Mazucheli, and B. Alves, "A Flexible Probability Model for Proportion Data: Unit Gumbel Type-II Distribution, Development, Properties, Different Method of Estimations and Applications," *Austrian Journal of Statistics* 52, no. 2 (2023): 116–140, https://doi.org/10.17713/ajs.v52i2.1407.

50. A. Shafiq, T. N. Sindhu, S. Dey, S. A. Lone, and T. A. Abushal, "Statistical Features and Estimation Methods for Half-Logistic Unit-Gompertz Type-I Model," *Mathematics* 11, no. 4 (2023): 1007, https://doi.org/10.3390/math11041007.

51. T. N. Sindhu, A. Shafiq, M. B. Riaz, and T. A. Abushal, "A Statistical Framework for a New Two-Parameter Unit Bilal Distribution With Application to Model Asymmetric Data," *Heliyon* 10, no. 19 (2024): e38340, https://doi.org/10.1016/j.heliyon.2024.e38340.

52. Y. Abdelall, G. Ismail, and H. Nagy, "A New Bounded Distribution: COVID-19 Application," *Egyptian Statistical Journal* 69, no. 1 (2025): 1–29, https://doi.org/10.21608/esju.2025.330520.1047.

53. J. A. Greenwood, J. M. Landwehr, N. C. Matalas, and J. R. Wallis, "Probability Weighted Moments: Definition and Relation to Parameters of Several Distributions Expressible in Inverse Form," *Water Resources Research* 15, no. 5 (1979): 1049–1054.

54. A. Rényi, "On Measures of Entropy and Information," *Proceedings of the Fourth Berkeley Symposium on Mathematical Statistics and Probability* 1 (1960): 547–561.

55. J. Havrda and F. Charvát, "Quantification Method of Classification Processes: Concept of Structural α-Entropy," *Kybernetika* 3, no. 1 (1967): 30–35.

56. C. Tsallis, "Possible Generalization of Boltzmann-Gibbs Statistics," *Journal of Statistical Physics* 52, no. 1–2 (1988): 479–487, https://doi.org/10.1007/BF01016429.

57. S. Arimoto, "Information-Theoretical Considerations on Estimation Problems," *Information and Control* 19, no. 3 (1971): 181–194, https://doi.org/10.1016/S0019-9958(71)90065-9.

58. M. K. Jha, S. Dey, R. Alotaibi, G. Alomani, and Y. T. Tripathi, "Multicomponent Stress-Strength Reliability Estimation Based on Unit Generalized Exponential Distribution," *Ain Shams Engineering Journal* 13, no. 5 (2022): 101627, https://doi.org/10.1016/j.asej.2021.10.022.

59. A. Pourdarvish, S. M. T. K. Mirmostafaee, and K. Naderi, "The Exponentiated Topp-Leone Distribution: Properties and Application," *Journal of Applied Environmental and Biological Sciences* 5, no. 7S (2015): 251–256.

60. W. S. Abu El Azm, E. M. Almetwally, S. N. AL-Aziz, A. A. A. H. El-Bagoury, R. Alharbi, and O. E. Abo-Kasem, "A New Transmuted Generalized Lomax Distribution: Properties and Applications to COVID-19 Data," *Computational Intelligence and Neuroscience* 2021 (2021): 5918511.

61. G. M. Cordeiro and R. S. Brito, "The Beta Power Distribution," *Brazilian Journal of Probability And Statistics* 26, no. 1 (2012): 88–112, https://doi.org/10.1214/10-BJPS124.

Appendix A

See Table A1.

TABLE A1 | Numerical values of the different entropy measures and their ABs and MSEs for set 1.

n	True value	δ_1		δ_2		Ré (−0.40489)		TS (−0.39680)		H–C (−0.55285)		AR (−0.39592)	
	Estimate	AB	MSE	AB	MSE	AB	MSE	AB	MSE	AB	MSE	AB	MSE
25	MLE	0.05340	0.02488	0.24693	0.40941	0.15783	0.04077	0.15059	0.03670	0.20981	0.07124	0.14981	0.03627
	KO	0.02500	0.02209	0.06776	0.19170	0.17053	0.04943	0.16258	0.04430	0.22652	0.08600	0.16172	0.04377
	LSE	0.01297	0.02684	0.06432	0.44842	0.17465	0.05201	0.16618	0.04642	0.23153	0.09011	0.16526	0.04584
	WLSE	0.01993	0.02510	0.09651	0.41082	0.16781	0.04780	0.15980	0.04274	0.22264	0.08297	0.15893	0.04222
	ADE	0.02725	0.02250	0.13136	0.37353	0.16513	0.04574	0.15736	0.04099	0.21924	0.07958	0.15652	0.04050
50	MLE	0.02336	0.00971	0.11835	0.15239	0.10927	0.01931	0.10456	0.01758	0.14567	0.03412	0.10405	0.01739
	KO	0.00860	0.00936	0.03317	0.07818	0.12242	0.02458	0.11708	0.02231	0.16312	0.04332	0.11650	0.02208
	LSE	0.00551	0.01274	0.04028	0.19524	0.12285	0.02455	0.11739	0.02225	0.16355	0.04319	0.11680	0.02201
	WLSE	0.00983	0.01111	0.05896	0.16686	0.11667	0.02214	0.11154	0.02010	0.15541	0.03901	0.11099	0.01988
	ADE	0.01123	0.01005	0.06724	0.15494	0.11615	0.02180	0.11107	0.01980	0.15475	0.03844	0.11052	0.01959
75	MLE	0.01429	0.00547	0.07256	0.08746	0.08907	0.01263	0.08533	0.01154	0.11889	0.02241	0.08493	0.01143
	KO	0.00672	0.00559	0.03038	0.05539	0.09982	0.01604	0.09559	0.01463	0.13319	0.02841	0.09514	0.01449
	LSE	0.00168	0.00698	0.02289	0.11871	0.10011	0.01626	0.09580	0.01481	0.13347	0.02875	0.09533	0.01466
	WLSE	0.00554	0.00602	0.03888	0.10034	0.09509	0.01463	0.09103	0.01334	0.12683	0.02590	0.09059	0.01321
	ADE	0.00579	0.00567	0.03997	0.09212	0.09449	0.01439	0.09047	0.01313	0.12605	0.02549	0.09003	0.01300
100	MLE	0.01272	0.00425	0.05338	0.05952	0.07624	0.00906	0.07312	0.00831	0.10188	0.01614	0.07278	0.00823
	KO	0.00628	0.00415	0.02247	0.03687	0.08717	0.01182	0.08357	0.01082	0.11643	0.02101	0.08318	0.01072
	LSE	0.00249	0.00536	0.01372	0.08045	0.08703	0.01164	0.08339	0.01065	0.11618	0.02068	0.08299	0.01055
	WLSE	0.00588	0.00463	0.02734	0.06788	0.08217	0.01044	0.07877	0.00956	0.10974	0.01857	0.07840	0.00947
	ADE	0.00621	0.00448	0.02919	0.06465	0.08206	0.01039	0.07866	0.00953	0.10960	0.01849	0.07830	0.00943
200	MLE	0.00549	0.00189	0.02550	0.02827	0.05363	0.00455	0.05146	0.00419	0.07170	0.00813	0.05122	0.00415
	KO	0.00347	0.00201	0.01300	0.01871	0.06076	0.00584	0.05830	0.00537	0.08122	0.01042	0.05803	0.00532
	LSE	0.00114	0.00256	0.00718	0.04065	0.06030	0.00575	0.05784	0.00528	0.08058	0.01024	0.05757	0.00523
	WLSE	0.00295	0.00213	0.01492	0.03314	0.05737	0.00518	0.05504	0.00476	0.07669	0.00923	0.05479	0.00471
	ADE	0.00261	0.00209	0.01358	0.03190	0.05724	0.00516	0.05492	0.00474	0.07651	0.00920	0.05466	0.00469

See Table A2

TABLE A2 | Numerical values of the different entropy measures and their ABs and MSEs for set 2.

n	True value	δ_1		δ_2		Ré (−0.61617)		TS (−0.59757)		H−C (−0.83257)		AR (−0.59555)	
	Estimate	AB	MSE	AB	MSE	AB	MSE	AB	MSE	AB	MSE	AB	MSE
25	ML	0.36686	0.96741	0.05869	0.02876	0.16576	0.04412	0.15509	0.03828	0.21608	0.07431	0.15395	0.03768
	KO	0.02098	0.08897	0.01186	0.01179	0.16889	0.04534	0.15825	0.03947	0.22049	0.07661	0.15712	0.03887
	LS	0.13045	0.98354	0.00439	0.02990	0.17638	0.04983	0.16494	0.04315	0.22981	0.08375	0.16372	0.04246
	WLS	0.16587	0.91525	0.01468	0.02728	0.17148	0.04742	0.16041	0.04110	0.22350	0.07979	0.15923	0.04046
	AD	0.20623	0.79717	0.02624	0.02610	0.16935	0.04582	0.15846	0.03976	0.22078	0.07718	0.15730	0.03914
50	ML	0.16187	0.30968	0.02955	0.01183	0.11537	0.02137	0.10824	0.01872	0.15081	0.03634	0.10748	0.01845
	KO	0.00556	0.05984	0.00748	0.00644	0.12120	0.02328	0.11378	0.02042	0.15853	0.03963	0.11299	0.02012
	LS	0.06454	0.41451	0.00531	0.01437	0.12417	0.02488	0.11644	0.02174	0.16224	0.04221	0.11562	0.02142
	WLS	0.08460	0.34898	0.01157	0.01253	0.11974	0.02320	0.11232	0.02029	0.15649	0.03940	0.11153	0.02000
	AD	0.09226	0.30718	0.01443	0.01182	0.11909	0.02271	0.11172	0.01989	0.15566	0.03860	0.11093	0.01960
75	ML	0.09919	0.16256	0.01874	0.00707	0.09399	0.01397	0.08825	0.01227	0.12296	0.02383	0.08764	0.01210
	KO	0.00910	0.03891	0.00657	0.00417	0.09735	0.01496	0.09147	0.01318	0.12744	0.02559	0.09084	0.01300
	LS	0.02996	0.21567	0.00279	0.00886	0.09984	0.01579	0.09375	0.01388	0.13062	0.02695	0.09310	0.01368
	WLS	0.04932	0.17876	0.00802	0.00765	0.09659	0.01481	0.09071	0.01303	0.12638	0.02529	0.09008	0.01284
	AD	0.05078	0.16306	0.00869	0.00721	0.09636	0.01471	0.09048	0.01293	0.12607	0.02511	0.08985	0.01275
100	ML	0.08186	0.11689	0.01402	0.00489	0.08161	0.01055	0.07662	0.00927	0.10676	0.01799	0.07609	0.00914
	KO	0.00421	0.02462	0.00322	0.00281	0.08661	0.01164	0.08137	0.01025	0.11337	0.01989	0.08081	0.01010
	LS	0.02614	0.15348	0.00144	0.00623	0.08829	0.01207	0.08291	0.01061	0.11552	0.02059	0.08233	0.01046
	WLS	0.04342	0.12828	0.00583	0.00533	0.08497	0.01129	0.07979	0.00992	0.11116	0.01926	0.07923	0.00978
	AD	0.04545	0.12290	0.00641	0.00516	0.08485	0.01123	0.07967	0.00987	0.11101	0.01917	0.07912	0.00973
200	ML	0.03551	0.05016	0.00641	0.00237	0.05702	0.00515	0.05358	0.00454	0.07466	0.00882	0.05321	0.00448
	KO	0.00884	0.01463	0.00298	0.00158	0.06014	0.00577	0.05652	0.00509	0.07875	0.00988	0.05613	0.00502
	LS	0.01239	0.07289	0.00072	0.00323	0.06180	0.00607	0.05807	0.00535	0.08090	0.01038	0.05767	0.00527
	WLS	0.02141	0.05840	0.00316	0.00269	0.05944	0.00560	0.05585	0.00494	0.07782	0.00958	0.05547	0.00487
	AD	0.01959	0.05626	0.00281	0.00260	0.05931	0.00558	0.05573	0.00492	0.07765	0.00955	0.05535	0.00485

See Table A3

TABLE A3 | Numerical values of the different entropy measures and their ABs and MSEs for set 3.

n	True value	δ_1		δ_2		Ré (−0.38956)		TS (−0.43008)		H−C (−0.73420)		AR (−0.41598)	
	Estimate	AB	MSE	AB	MSE	AB	MSE	AB	MSE	AB	MSE	AB	MSE
25	ML	0.10072	0.08191	0.27327	0.55313	0.15975	0.04703	0.20527	0.08657	0.35041	0.25227	0.18862	0.07026
	KO	0.04484	0.15533	0.05854	0.31544	0.17961	0.06759	0.23620	0.14103	0.40321	0.41099	0.21518	0.10913
	LS	0.02762	0.08723	0.04758	0.58054	0.20319	0.09479	0.27762	0.29193	0.47393	0.85074	0.24898	0.18696
	WLS	0.03971	0.08129	0.08888	0.53128	0.18559	0.07289	0.24644	0.16474	0.42069	0.48009	0.22368	0.12284
	AD	0.05335	0.07217	0.13611	0.50253	0.17570	0.06190	0.22998	0.12790	0.39259	0.37274	0.20988	0.09899
50	ML	0.04444	0.03029	0.13392	0.21739	0.10739	0.01961	0.13417	0.03205	0.22903	0.09341	0.12453	0.02717
	KO	0.01335	0.02805	0.02924	0.11630	0.12149	0.02668	0.15312	0.04563	0.26139	0.13297	0.14167	0.03805
	LS	0.01277	0.04009	0.03541	0.26797	0.12805	0.03020	0.16262	0.05262	0.27760	0.15335	0.15007	0.04359
	WLS	0.02011	0.03457	0.06007	0.23212	0.11842	0.02488	0.14921	0.04199	0.25472	0.12236	0.13808	0.03519
	AD	0.02289	0.03100	0.07174	0.21825	0.11678	0.02378	0.14679	0.03978	0.25059	0.11592	0.13596	0.03344
75	ML	0.02720	0.01667	0.08317	0.12749	0.08659	0.01260	0.10718	0.02002	0.18297	0.05834	0.09980	0.01714
	KO	0.00857	0.01645	0.02433	0.08268	0.09669	0.01633	0.12038	0.02647	0.20550	0.07713	0.11186	0.02250
	LS	0.00480	0.02152	0.01964	0.16432	0.10160	0.01860	0.12725	0.03132	0.21722	0.09129	0.11800	0.02624
	WLS	0.01150	0.01832	0.04042	0.14088	0.09438	0.01554	0.11753	0.02533	0.20063	0.07383	0.10920	0.02148
	AD	0.01215	0.01710	0.04288	0.13144	0.09335	0.01506	0.11611	0.02439	0.19821	0.07107	0.10793	0.02073
100	ML	0.02360	0.01268	0.06163	0.08754	0.07291	0.00857	0.08964	0.01326	0.15302	0.03864	0.08366	0.01146
	KO	0.00749	0.01133	0.01555	0.05128	0.08339	0.01125	0.10288	0.01763	0.17562	0.05138	0.09590	0.01516
	LS	0.00547	0.01623	0.01125	0.11372	0.08569	0.01201	0.10611	0.01902	0.18114	0.05543	0.09879	0.01630
	WLS	0.01138	0.01386	0.02876	0.09699	0.07964	0.01023	0.09825	0.01599	0.16773	0.04661	0.09159	0.01377
	AD	0.01211	0.01337	0.03145	0.09329	0.07942	0.01014	0.09795	0.01583	0.16720	0.04613	0.09132	0.01363
200	ML	0.01021	0.00558	0.02898	0.04206	0.05123	0.00424	0.06265	0.00643	0.10696	0.01873	0.05858	0.00559
	KO	0.00458	0.00586	0.00988	0.02975	0.05709	0.00541	0.06996	0.00828	0.11943	0.02412	0.06537	0.00718
	LS	0.00254	0.00775	0.00586	0.05821	0.05805	0.00549	0.07122	0.00841	0.12157	0.02452	0.06652	0.00730
	WLS	0.00566	0.00636	0.01571	0.04817	0.05489	0.00484	0.06722	0.00737	0.11475	0.02147	0.06282	0.00640
	AD	0.00513	0.00620	0.01432	0.04653	0.05476	0.00483	0.06705	0.00734	0.11447	0.02140	0.06267	0.00638

See Table A4

TABLE A4 | Numerical values of the different entropy measures and their ABs and MSEs for set4.

n	True value	δ_1		δ_2		Ré (−0.54937)		TS (−0.63223)		H−C (−1.07929)		AR (−0.60289)	
	Estimate	AB	MSE	AB	MSE	AB	MSE	AB	MSE	AB	MSE	AB	MSE
25	ML	0.42082	1.26243	0.07633	0.04901	0.17225	0.05401	0.23837	0.11824	0.40692	0.34456	0.21362	0.09022
	KO	0.03616	0.16497	0.01603	0.02011	0.18521	0.06616	0.25917	0.19540	0.44244	0.56944	0.23095	0.12881
	LS	0.15341	1.27553	0.00520	0.05103	0.22446	0.12020	0.34359	0.93024	0.58654	0.71092	0.29423	0.37926
	WLS	0.19306	1.18734	0.01871	0.04652	0.20430	0.08595	0.29358	0.23877	0.50117	0.69584	0.25935	0.16526
	AD	0.23793	1.03226	0.03382	0.04448	0.19141	0.06930	0.26937	0.16560	0.45985	0.48258	0.23992	0.12209
50	ML	0.18549	0.39709	0.03852	0.02021	0.11902	0.02370	0.15993	0.04506	0.27302	0.13131	0.14486	0.03628
	KO	0.01904	0.07098	0.01196	0.00960	0.12845	0.02741	0.17248	0.05241	0.29445	0.15272	0.15625	0.04210
	LS	0.07606	0.53152	0.00670	0.02455	0.13600	0.03243	0.18517	0.06463	0.31610	0.18833	0.16695	0.05119
	WLS	0.09825	0.44642	0.01492	0.02140	0.12802	0.02817	0.17322	0.05488	0.29570	0.15993	0.15652	0.04381
	AD	0.10661	0.39221	0.01866	0.02019	0.12549	0.02685	0.16942	0.05186	0.28921	0.15113	0.15320	0.04153
75	ML	0.11350	0.20727	0.02445	0.01208	0.09577	0.01520	0.12779	0.02793	0.21815	0.08140	0.11604	0.02277
	KO	0.01381	0.04655	0.00882	0.00660	0.10290	0.01710	0.13695	0.03122	0.23379	0.09098	0.12446	0.02550
	LS	0.03578	0.27607	0.00349	0.01515	0.10624	0.01892	0.14257	0.03556	0.24339	0.10363	0.12921	0.02876
	WLS	0.05735	0.22807	0.01036	0.01308	0.10067	0.01690	0.13464	0.03130	0.22985	0.09121	0.12216	0.02545
	AD	0.05883	0.20742	0.01124	0.01232	0.10019	0.01668	0.13394	0.03086	0.22865	0.08993	0.12155	0.02510
100	ML	0.09333	0.14814	0.01832	0.00836	0.08295	0.01104	0.11037	0.02007	0.18842	0.05848	0.10033	0.01642
	KO	0.01722	0.03820	0.00699	0.00507	0.09149	0.01325	0.12162	0.02402	0.20761	0.06999	0.11058	0.01967
	LS	0.03068	0.19483	0.00178	0.01066	0.09188	0.01348	0.12265	0.02469	0.20937	0.07195	0.11136	0.02016
	WLS	0.04998	0.16255	0.00755	0.00912	0.08726	0.01221	0.11627	0.02224	0.19848	0.06481	0.10564	0.01819
	AD	0.05219	0.15563	0.00830	0.00883	0.08682	0.01208	0.11564	0.02198	0.19741	0.06407	0.10508	0.01798
200	ML	0.04052	0.06336	0.00836	0.00406	0.05820	0.00545	0.07701	0.00967	0.13146	0.02817	0.07014	0.00798
	KO	0.01201	0.02194	0.00399	0.00267	0.06348	0.00647	0.08399	0.01151	0.14338	0.03353	0.07650	0.00949
	LS	0.01457	0.09243	0.00088	0.00553	0.06417	0.00660	0.08510	0.01181	0.14527	0.03442	0.07745	0.00972
	WLS	0.02462	0.07390	0.00408	0.00461	0.06133	0.00600	0.08122	0.01067	0.13865	0.03109	0.07395	0.00880
	AD	0.02254	0.07112	0.00363	0.00445	0.06115	0.00597	0.08098	0.01063	0.13824	0.03098	0.07373	0.00877

Appendix B

See Appendix B

Coding in R of Lorenz and Bonferroni curves

```
library(ineq)
# Define parameter sets with distinct colors
params < - list
(    list(delta1 = 0.5, delta2 = 2.4, color = "blue"),
   list(delta1 = 1.4, delta2 = 0.8, color = "red"),
   list(delta1 = 0.3, delta2 = 0.3, color = "green"),
   list(delta1 = 2.5, delta2 = 2.5, color = "gold"),
   list(delta1 = 1.5, delta2 = 2.3, color = "purple")).
# Basic Probability Distribution Functions (PDF, CDF, Quantile)
fx < - function(x, delta1, delta2) {
   delta1 * delta2 * (1 − x)^(delta2 − 1) * (1 − (1 − x)^delta2)^(delta1 − 1)
}
Fx < - function(x, delta1, delta2) {
   (1 − (1 − x)^delta2)^delta1
```

```
}
Qx < - function(d, delta1, delta2) {
  1 – (1 – d^(1/delta1))^(1/delta2)
}
# Functions for Inequality Curves
lorenz_curve < - function(samples) {
  sorted_samples < - sort(samples)
  cum_samples < - cumsum(sorted_samples)
  total < - sum(sorted_samples)
  L < - cum_samples/total
  p < - seq(1/length(samples), 1, length.out = length(samples))
  list(p = p, L = L)
}
bonferroni_curve < - function(lorenz_curve) {
B < - lorenz_curve$L/lorenz_curve$p
  list(p = lorenz_curve$p, B = B)}
# Sample Generation
generate_samples < - function(param) {
  n < - 10,000
  u < - runif(n)
  Qx(u, param$delta1, param$delta2)
}
# Plotting Setup
par(mfrow = c(1, 2), cex.main = 1.2, cex.lab = 1.5, cex.axis = 1.4,
  mar = c(5, 5, 4, 2), mgp = c(3.5, 1, 0))
# Plotting Lorenz Curves
plot(NULL, type = "n", xlim = c(0, 1), ylim = c(0, 1),
     xlab = "t", ylab = bquote({{L}}[F](t)), main = "Lorenz Curve", lwd = 2)
for (param in params) {
  samples < - generate_samples(param)
  lc < - lorenz_curve(samples)
  lines(lc$p, lc$L, col = param$color, lwd = 3.5)}
segments(0, 0, 1, 1, col = "black", lty = 1, lwd = 3.5)
text(0.3, 0.32, expression(L(t) == t), pos = 2, cex = 1.2)
legend("topleft", legend = sapply(params, function(p) bquote(delta [1] == (p$delta1) ~ delta [2] == (p$delta2))),
  col = sapply(params, function(p) p$color), lwd = 4, bty = "n", cex = 1.2)
# Plotting Bonferroni Curves
plot(NULL, type = "n", xlim = c(0, 1), ylim = c(0, 1),
     xlab = "t", ylab = bquote({{B}}[F](t)), main = "Bonferroni Curve", lwd = 2).
for (param in params) {
  samples < - generate_samples(param).
  lc < - lorenz_curve(samples).
  bc < - bonferroni_curve(lc).
  lines(bc$p, bc$B, col = param$color, lwd = 3.5)}
segments(0, 0, 1, 1, col = "black", lty = 1, lwd = 3.5)
text(0.3, 0.3, expression(B(t) == t), pos = 4, cex = 1.2)
```

```
legend("topleft", legend = sapply(params, function(p) bquote(delta [1] == (p$delta1) ~ delta [2] == (p$delta2))),
       col = sapply(params, function(p) p$color), lwd = 4, bty = "n", cex = 1.2)
########################### Goodness of Fit test ################################
#################clean up everything###############
remove(list = objects())
options(warn = -1)
#################Packages###############
library(stats4)
library(bbmle)
library(MASS)
library(AdequacyModel)
library(ggplot2)
########################### PDF and CDF of Distribution
##############define pdf and cdf for Unit inverse Exponentiated Pareto (UIEP) Distribution################
Pdf_UIEP <- function(parm,x){
  delta1 <- parm[1]
  delta2 <- parm[2]
  Pdf_UIEP <- delta1 * delta2 * (1 - x)^(delta2 - 1) * (1 - (1 - x)^delta2)^(delta1 - 1)}
Cdf_UIEP <- function(parm,x){
  delta1 <- parm[1]
  delta2 <- parm[2]
  Cdf_UIEP <- (1 - (1 - x)^delta2)^delta1}
#############define pdf and cdf for Unit Exponential Pareto (UEP) Distribution###############
Pdf_UEP <- function(parm,x){
  delta1 <- parm[1]
  delta2 <- parm[2]
  delta3 <- parm[3]
  Pdf_UEP <- (delta1 * delta3)/delta2*(x/(delta2 * (1 - x)))^(delta1 - 1)*exp(-delta3 * (x/(delta2 * (1 - x)))^delta1)}
Cdf_UEP <- function(parm,x){
  delta1 <- parm[1]
  delta2 <- parm[2]
  delta3 <- parm[3]
  Cdf_UEP <- 1 - exp(-delta3 * (x/(delta2 * (1 - x)))^delta1)}
########define pdf and cdf for unit exponentiated Lomax (UEL) Distribution
Pdf_UEL <- function(parm,x){
  delta1 <- parm[1]
  delta2 <- parm[2]
  delta3 <- parm[3]
  Pdf_UEL <- (delta1 * delta2 * delta3/x) * (1 - delta1 * log(x))^(-delta2 - 1) * (1 - (1 - delta1 * log(x))^(-delta2))^(delta3 - 1)}
Cdf_UEL <- function(parm,x){
  delta1 <- parm[1]
  delta2 <- parm[2]
  delta3 <- parm[3]
  Cdf_UEL <- (1-((1 - (1 - delta1 * log(x))^(-delta2))^(delta3)))}
#############define pdf and cdf for Unit-Exponentiated Half-Logistic (UEHL) Distribution ##########
Pdf_UEHL<- function(parm,x){
```

```
  delta1 < - parm[1]
  delta2 < - parm[2]
  Pdf_UEHL<- (2 * delta1 * delta2 * x^(delta2 − 1))/((1 + x^delta2)^2) * ((1 − x^delta2)/(1 + x^delta2))^(delta1 − 1)}
Cdf_UEHL<- function(parm,x){
  delta1 < - parm[1]
  delta2 < - parm[2]
  Cdf_UEHL < - 1 − ((1 − x^delta2)/(1 + x^delta2))^(delta1)}
############define pdf and cdf for umaraswamy Distribution (KW) Distribution #################.
Pdf_KW < - function(parm,x){
  delta1 < - parm[1]
  delta2 < - parm[2]
  Pdf_KW < - (delta1*delta2)*(x^(delta1 − 1))*((1 − (x^delta1))^(delta2 − 1))}
Cdf_KW < - function(parm,x){
  delta1 < - parm[1]
  delta2 < - parm[2]
  Cdf_KW < - 1 − ((1 − (x^delta1))^delta2)}
############## define pdf and cdf of Exponentiated Topp-Leone (ETL) Distribution
Pdf_ETL < - function(parm,x){
  delta1 < - parm[1]
  delta2 < - parm[2]
  Pdf_ETL < -2 * delta1 * delta2 * (1 − x) * (x * (2 − x))^(delta1 − 1) * (1 − x^delta1 * (2 − x)^delta1)^(delta2 − 1)}
Cdf_ETL < - function(parm,x){
  delta1 < - parm[1]
  delta2 < - parm[2]
  Cdf_ETL < - 1 − (1 − x^delta1 * (2 − x)^delta1)^(delta2)}
#############define pdf and cdf for unit log logistic (ULL) distribution ###############
Pdf_ULL < - function(parm,x){
  delta1 < - parm[1]
  delta2 < - parm[2]
Pdf_ULL < - (delta1/(x*delta2^delta1)) * (−log(x))^(delta1-1) * (1 + (−log(x)/delta2)^delta1)^(−2)}
Cdf_ULL < - function(parm,x){
  delta1 < - parm[1]
  delta2 < - parm[2]
  Cdf_ULL < - (1 + (−log(x)/delta2)^delta1)^(−1)}
#############define pdf and cdf for unit power Lomax (UPL) Distribution###############
Pdf_UPL < - function(parm,x){
  delta1 < - parm [1]
  delta2 < - parm [2]
  delta3 < - parm [3]
Pdf_UPL < - (delta1*delta2/(x*delta3))*((−log(x))^(delta1-1))*((1 + (1/delta3)*(−log(x))^delta1)^(−delta2 − 1))}
Cdf_UPL < - function(parm,x){
  delta1 < - parm[1]
  delta2 < - parm[2]
  delta3 < - parm[3]
    Cdf_UPL < - (1 + (1/delta3)*(−log(x))^delta1)^(−delta2)}
######################### Loglikelihood function ################################
```

```
LL_UIEP < - function(delta1,delta2){−sum(log(Pdf_UIEP(c(delta1,delta2),x)))}
LL_UEP < - function(delta1,delta2,delta3){−sum(log(Pdf_UEP(c(delta1,delta2,delta3),x)))}
LL_UEL < - function(delta1,delta2,delta3){−sum(log(Pdf_UEL(c(delta1,delta2,delta3),x)))}
LL_UEHL < - function(delta1,delta2){−sum(log(Pdf_UEHL(c(delta1,delta2),x)))}
LL_KW < - function(delta1,delta2){−sum(log(Pdf_KW(c(delta1,delta2),x)))}
LL_ETL < - function(delta1,delta2){−sum(log(Pdf_ETL(c(delta1,delta2),x)))}
LL_ULL < - function(delta1,delta2){−sum(log(Pdf_ULL(c(delta1,delta2),x)))}
LL_UPL < - function(delta1,delta2,delta3){−sum(log(Pdf_UPL(c(delta1,delta2,delta3),x)))}
############################## Real data ############################
#####################################################################################
x < - c(0.0903296, 0.2036540, 0.2043140, 0.2808870, 0.1976530, 0.3286410,
      0.1486220, 0.1623940, 0.2627270, 0.1794550, 0.3266350, 0.2300810,
      0.1833120, 0.1509440, 0.2000710, 0.1918020, 0.1541920, 0.4641250,
      0.1170630, 0.1481410, 0.1448100, 0.1330830, 0.2760160, 0.4204770,
      0.1224170, 0.2285950, 0.1138520, 0.2252140, 0.1769690, 0.2007440,
      0.1670450, 0.2316230, 0.2910290, 0.3412730, 0.4387120, 0.2626510,
      0.1896510, 0.1725670, 0.2400770, 0.3116460, 0.1635860, 0.1824530,
      0.1641270, 0.1534810, 0.1618650, 0.2760160, 0.2538320, 0.2004470)
######## Maximum likelihood estimation for many distributions ##############
#####################################################################################
fit_UIEP < - mle2(minuslog = LL_UIEP,start = list(delta1 = 0.8,delta2 = 0.9),data = list(x), method = "BFGS")
fit_UEP < - mle2(minuslog = LL_UEP,start = list(delta1 = 0.8,delta2 = 0.5,delta3 = 0.1),data = list(x), method = "BFGS")
fit_UEL < - mle2(minuslog = LL_UEL,start = list(delta1 = 0.5,delta2 = 0.2,delta3 = 0.9),data = list(x), method = "BFGS")
fit_UEHL < - mle2(minuslog = LL_UEHL,start = list(delta1 = 0.08,delta2 = 0.01),data = list(x), method = "BFGS")
fit_KW < - mle2(minuslog = LL_KW,start = list(delta1 = 0.3,delta2 = 0.1),data = list(x), method = "BFGS")
fit_ETL < - mle2(minuslog = LL_ETL,start = list(delta1 = 0.2,delta2 = 0.4),data = list(x), method = "BFGS")
fit_ULL < - mle2(minuslog = LL_ULL,start = list(delta1 = 0.1,delta2 = 0.1),data = list(x), method = "BFGS")
fit_UPL < - mle2(minuslog = LL_UPL,start = list(delta1 = 0.8,delta2 = 0.9,delta3 = 0.1),data = list(x), method = "BFGS")
############Goodness of fit test###############
gof.test_UIEP < - goodness.fit(Pdf_UIEP,Cdf_UIEP,starts = c(coef(fit_UIEP)),data = x, method = "BFGS", domain = c(0, 1))
gof.test_UEP < - goodness. fit(Pdf_UEP,Cdf_UEP,starts = c(coef(fit_UEP)),data = x, method = "BFGS", domain = c(0, 1))
gof.test_UEL < - goodness. fit(Pdf_UEL,Cdf_UEL,starts = c(coef(fit_UEL)),data = x, method = "BFGS", domain = c(0, 1))
gof.test_UEHL < - goodness.fit(Pdf_UEHL,Cdf_UEHL,starts = c(coef(fit_UEHL)),data = x, method = "BFGS", domain = c(0, 1))
gof.test_KW < - goodness. fit(Pdf_KW,Cdf_KW,starts = c(coef(fit_KW)),data = x, method = "BFGS", domain = c(0, 1))
gof.test_ETL < - goodness. fit(Pdf_ETL,Cdf_ETL,starts = c(coef(fit_ETL)),data = x, method = "BFGS", domain = c(0,1))
gof.test_ULL < - goodness. fit(Pdf_ULL,Cdf_ULL,starts = c(coef(fit_ULL)),data = x, method = "BFGS", domain = c(0, 1))
gof.test_UPL < - goodness. fit(Pdf_UPL,Cdf_UPL,starts = c(coef(fit_UPL)),data = x, method = "BFGS", domain = c(0, 1))
################## Results#####################
Name < - c("UIEP","UEP","UEL","UEHL","KW","ETL","ULL","UPL")
ParmI < - c(gof.test_UIEP$mle[1],gof.test_UEP$mle[1]
      ,gof.test_UEL$mle[1]
      ,gof.test_UEHL$mle[1]
      ,gof.test_KW$mle[1]
      ,gof.test_ETL$mle[1]
      ,gof.test_ULL$mle[1]
      ,gof.test_UPL$mle[1])
```

```
ParmII < - c(gof.test_UIEP$mle[2]
        ,gof.test_UEP$mle[2]
        ,gof.test_UEL$mle[2]
        ,gof.test_UEHL$mle[2]
        ,gof.test_KW$mle[2]
        ,gof.test_ETL$mle[2]
        ,gof.test_ULL$mle[2]
        ,gof.test_UPL$mle[2])
ParmIII < - c(gof.test_UIEP$mle[3]
        ,gof.test_UEP$mle[3]
        ,gof.test_UEL$mle[3]
        ,gof.test_UEHL$mle[3]
        ,gof.test_KW$mle[3]
        ,gof.test_ETL$mle[3]
        ,gof.test_ULL$mle[3]
        ,gof.test_UPL$mle[3])
St.Er_ParmI < - c(gof.test_UIEP$Erro[1]
            ,gof.test_UEP$Erro[1]
            ,gof.test_UEL$Erro[1]
            ,gof.test_UEHL$Erro[1]
            ,gof.test_KW$Erro[1]
            ,gof.test_ETL$Erro[1]
            ,gof.test_ULL$Erro[1]
            ,gof.test_UPL$Erro[1])
St.Er_ParmII < - c(gof.test_UIEP$Erro [2],gof.test_UEP$Erro[2]
            ,gof.test_UEL$Erro[2]
            ,gof.test_UEHL$Erro[2]
            ,gof.test_KW$Erro[2]
            ,gof.test_ETL$Erro[2]
            ,gof.test_ULL$Erro[2]
            ,gof.test_UPL$Erro[2])
St.Er_ParmIII < - c(gof.test_UIEP$Erro[3],gof.test_UEP$Erro[3]
            ,gof.test_UEL$Erro[3]
            ,gof.test_UEHL$Erro[3]
            ,gof.test_KW$Erro[3],gof.test_ETL$Erro[3]
            ,gof.test_ULL$Erro[3]
            ,gof.test_UPL$Erro[3])
ML < - c(gof.test_UIEP$Value,gof.test_UEP$Value
        ,gof.test_UEL$Value
        ,gof.test_UEHL$Value
        ,gof.test_KW$Value,gof.test_ETL$Value
        ,gof.test_ULL$Value
        ,gof.test_UPL$Value)
AIC < - c(gof.test_UIEP$AIC,gof.test_UEP$AIC
        ,gof.test_UEL$AIC
        ,gof.test_UEHL$AIC
```

```
        ,gof.test_KW$AIC,gof.test_ETL$AIC
        ,gof.test_ULL$AIC
        ,gof.test_UPL$AIC)
BIC < - c(gof.test_UIEP$BIC,gof.test_UEP$BIC
        ,gof.test_UEL$BIC
        ,gof.test_UEHL$BIC
        ,gof.test_KW$BIC,gof.test_ETL$BIC
        ,gof.test_ULL$BIC
        ,gof.test_UPL$BIC)
CAIC < - c(gof.test_UIEP$CAIC,gof.test_UEP$CAIC
        ,gof.test_UEL$CAIC
        ,gof.test_UEHL$CAIC
        ,gof.test_KW$CAIC,gof.test_ETL$CAIC
        ,gof.test_ULL$CAIC
        ,gof.test_UPL$CAIC)
HQIC < - c(gof.test_UIEP$HQIC,gof.test_UEP$HQIC
        ,gof.test_UEL$HQIC,gof.test_UEHL$HQIC
        ,gof.test_KW$HQIC,gof.test_ETL$HQIC
        ,gof.test_ULL$HQIC
        ,gof.test_UPL$HQIC)
KS < - c(gof.test_UIEP$KS$statistic,gof.test_UEP$KS$statistic
        ,gof.test_UEL$KS$statistic,gof.test_UEHL$KS$statistic
        ,gof.test_KW$KS$statistic,gof.test_ETL$KS$statistic
        ,gof.test_ULL$KS$statistic
        ,gof.test_UPL$KS$statistic)
P_value < - c(gof.test_UIEP$KS$p. value,gof.test_UEP$KS$p. value
        ,gof.test_UEL$KS$p. value,gof.test_UEHL$KS$p. value
        ,gof.test_KW$KS$p. value,gof.test_ETL$KS$p. value
        ,gof.test_ULL$KS$p. value
        ,gof.test_UPL$KS$p. value)
W < - c(gof.test_UIEP$W,gof.test_UEP$W
      ,gof.test_UEL$W
      ,gof.test_UEHL$W
      ,gof.test_KW$W
      ,gof.test_ETL$W
      ,gof.test_ULL$W
      ,gof.test_UPL$W)
A < - c(gof.test_UIEP$A,gof.test_UEP$A
      ,gof.test_UEL$A
      ,gof.test_UEHL$A
      ,gof.test_KW$A
      ,gof.test_ETL$A
      ,gof.test_ULL$A
      ,gof.test_UPL$A)
ResultsofMLE < - data.frame(Name,ParmI,ParmII,ParmIII,St.Er_ParmI,St.Er_ParmII,St.Er_ParmIII)
Resultsofgof < - data. frame(Name,ML,AIC,BIC,CAIC,HQIC,W,A,KS,P_value)
```

```
##########Graph of Histogram##########
data < - x
# Set larger font sizes globally
par(cex.axis = 1.2, cex.lab = 1.2, cex.main = 1.5, mfrow = c(1, 2), mar = c(5, 5, 4, 2),las = 1)
y < - seq(0, max(x), length. out = 1000)
hist(data, probability = TRUE,col = "skyblue",ylim = c(0,7),xlim = c(min(x),max(x)), ylab = "h(y)",xlab = "y",main = "")
lines(y, Pdf_UIEP(par < - gof.test_UIEP$mle,y), col = c(2),lwd = 3.5)
lines(y, Pdf_UEP(par < - gof.test_UEP$mle,y),col = c(3),lwd = 3.5)
lines(y, Pdf_UEL(par < - gof.test_UEL$mle,y), col = c(4),lwd = 3.5)
lines(y, Pdf_UEHL(par < - gof.test_UEHL$mle,y), col = c(5),lwd = 3.5)
lines(y, Pdf_KW(par < - gof.test_KW$mle,y), col = c(6),lwd = 3.5)
lines(y, Pdf_ETL(par < - gof.test_ETL$mle,y), col = c(7),lwd = 3.5)
lines(y, Pdf_ULL(par < - gof.test_ULL$mle,y), col = c(8),lwd = 3.5)
lines(y, Pdf_UPL(par < - gof.test_UPL$mle,y), col = "navy",lwd = 3.5)
legend(0.28,7,horiz = F, c("UIEP","UEP","UEL","UEHL","KW","ETL","ULL","UPL"), cex = 0.85,lty = 1,col = c(2,3,4,5,6,7,8,"navy"),lwd = 3.5)
#########Graph of Empirical cdf###########
plot(ecdf(data),verticals = TRUE, main = "",ylab = "H(y)",xlab = "y")
lines(y,Cdf_UIEP(par < - gof.test_UIEP$mle,y), col = c(2),lwd = 3.5)
lines(y, Cdf_UEP(par < - gof.test_UEP$mle,y),col = c(3),lwd = 3.5)
lines(y, Cdf_UEL(par < - gof.test_UEL$mle,y), col = c(4),lwd = 3.5)
lines(y, Cdf_UEHL(par < - gof.test_UEHL$mle,y), col = c(5),lwd = 3.5)
lines(y, Cdf_KW(par < - gof.test_KW$mle,y), col = c(6),lwd = 3.5)
lines(y, Cdf_ETL(par < - gof.test_ETL$mle,y), col = c(7),lwd = 3.5)
lines(y, Cdf_ULL(par < - gof.test_ULL$mle,y), col = c(8),lwd = 3.5)
lines(y, Cdf_UPL(par < - gof.test_UPL$mle,y), col = "navy",lwd = 3.5)
legend(0.25,0.58, c("Empirical","UIEP","UEP","UEL","UEHL","KW","ETL","ULL","UPL"), cex = 0.85,lty = 1,col = c(1,2,3,4,5,6,7,8,"navy"),lwd = 3.5)
################## pp plot #################
par(cex.axis = 1.3, cex.lab = 1.3, cex.main = 1.3, mfrow = c(2, 4), mar = c(5, 5, 4, 2))
p < - (rank(x))/(length(x) + 1)
plot(Cdf_UIEP(par < - gof.test_UIEP$mle,x),p,type = "p",pch = 1,xlim = c(0,1),ylim = c(0,1),col = 2,xlab = "Obs",ylab = "Exp", lwd = 4, main = "UIEP")
par(new = TRUE)
segments(0,0,1,1, lwd = 2)

p < - (rank(x))/(length(x) + 1)
plot(Cdf_UEP(par < - gof.test_UEP$mle,x),p,type = "p",pch = 1,xlim = c(0,1),ylim = c(0,1),col = 3,xlab = "Obs",ylab = "Exp", lwd = 4, main = "UEP")
par(new = TRUE)
segments(0,0,1,1, lwd = 2)

p < - (rank(x))/(length(x) + 1)
plot(Cdf_UEL(par < − gof.test_UEL$mle,x),p,type = "p",pch = 1,xlim = c(0,1),ylim = c(0,1),col = 4,xlab = "Obs",ylab = "Exp", lwd = 4, main = "UEL")
par(new = TRUE)
segments(0,0,1,1, lwd = 2)

p < - (rank(x))/(length(x) + 1)
plot(Cdf_UEHL(par < - gof.test_UEHL$mle,x),p,type = "p",pch = 1,xlim = c(0,1),ylim = c(0,1),col = 5,xlab = "Obs",ylab = "Exp", lwd = 4,
main = "UEHL")
```

```
par(new = TRUE)
segments(0,0,1,1, lwd = 2)

p < - (rank(x))/(length(x) + 1)
plot(Cdf_KW(par < - gof.test_KW$mle,x),p,type = “p”,pch = 1,xlim = c(0,1),ylim = c(0,1),col = 6,xlab = “Obs”,ylab = “Exp”, lwd = 4, main = “KW”)
par(new = TRUE)
segments(0,0,1,1, lwd = 2)

p < - (rank(x))/(length(x) + 1)
plot(Cdf_ETL(par < - gof.test_ETL$mle,x),p,type = “p”,pch = 1,xlim = c(0,1),ylim = c(0,1),col = 7,xlab = “Obs”,ylab = “Exp”, lwd = 4, main = “ETL”)
par(new = TRUE)
segments(0,0,1,1, lwd = 2)

p < - (rank(x))/(length(x) + 1)
plot(Cdf_ULL(par < - gof.test_ULL$mle,x),p,type = “p”,pch = 1,xlim = c(0,1),ylim = c(0,1),col = 8,xlab = “Obs”,ylab = “Exp”, lwd = 4, main = “ULL”)
par(new = TRUE)
segments(0,0,1,1, lwd = 2)
p < - (rank(x))/(length(x) + 1)
plot(Cdf_UPL(par < - gof.test_UPL$mle,x),p,type = “p”,pch = 1,xlim = c(0,1),ylim = c(0,1),col = “navy”,xlab = “Obs”,ylab = “Exp”, lwd = 4,
main = “UPL”)
par(new = TRUE)
segments(0,0,1,1, lwd = 2)
ResultsofMLE
Resultsofgof
```